

AD-A061 252

CALSPAN CORP BUFFALO N Y

F/G 7/4

RELATIVE TRANSITION PROBABILITY AND PRESSURE BROADENING PARAMET--ETC(U)

JUL 78 D W BOYER, W H WURSTER, A L RUSSO

F33615-75-C-3082

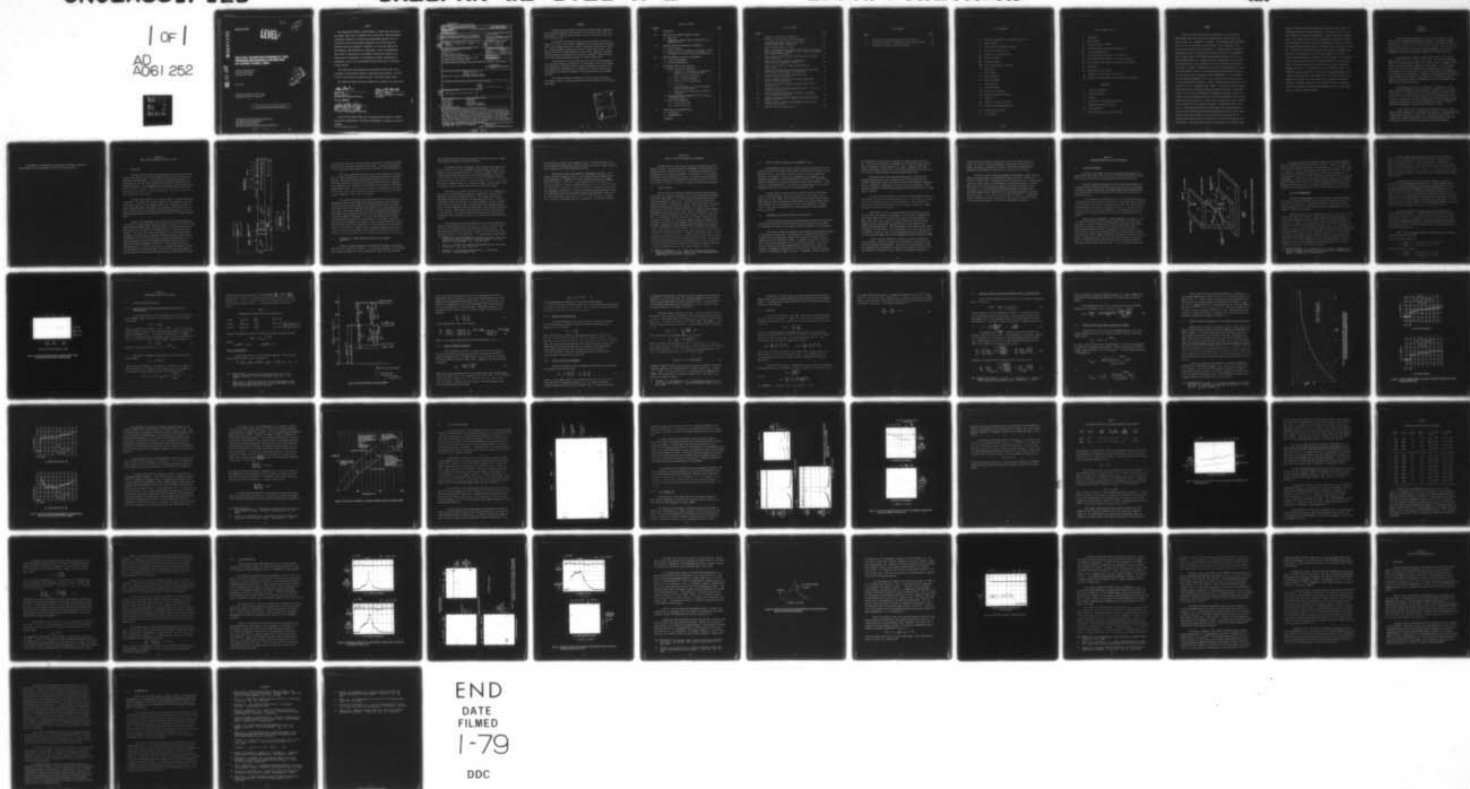
UNCLASSIFIED

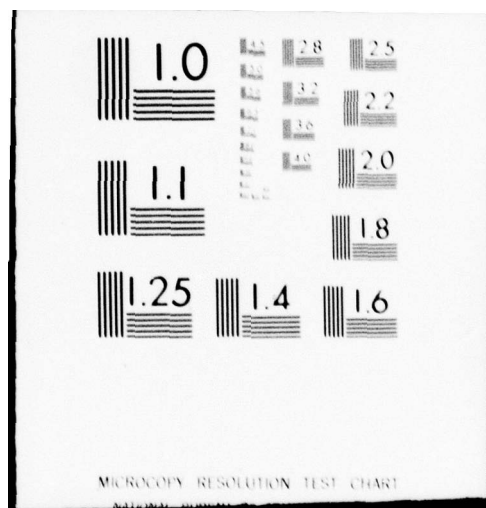
CALSPAN-WB-5726-A-3

AEFI -TR-7A-A2

All

1 of 1  
AD  
A061 252





AD A061252

DDC FILE COPY

AFFDL-TR-78-82

LEVEL II

B.S.

# RELATIVE TRANSITION PROBABILITY AND PRESSURE BROADENING PARAMETERS OF COPPER ATOMIC LINES

CALSPAN CORPORATION  
4455 GENESEE STREET  
BUFFALO, NEW YORK

JULY 1978

TECHNICAL REPORT AFFDL-TR-78-82  
Final Report April 1975 - August 1977

NOV 16 1978  
RECEIVED

Approved for public release; distribution unlimited.

AIR FORCE FLIGHT DYNAMICS LABORATORY  
AIR FORCE SYSTEMS COMMAND  
UNITED STATES AIR FORCE  
WRIGHT-PATTERSON AIR FORCE BASE, OHIO 45433

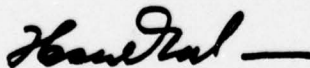
78 10 27 024

## NOTICE

When Government Drawings, specifications, or other data are used for any purpose other than in connection with a definitely related Government procurement operation, the United States Government thereby incurs no responsibility nor any obligation whatsoever; and the fact that the government may have formulated, furnished, or in any way supplied the said drawings, specifications, or other data, is not to be regarded by implication or otherwise as in any manner licensing the holder or any other person or corporation, or conveying any rights or permission to manufacture, use, or sell any patented invention that may in any way be related thereto.

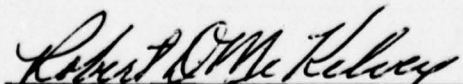
This report has been reviewed by the Information Office (OI) and is releasable to the National Technical Information Service (NTIS). At NTIS, it will be available to the general public, including foreign nations.

This Technical Report has been reviewed and is approved for publication.



HSUE-FU LEE  
Project Engineer  
Experimental Engineering Branch

FOR THE COMMANDER



ROBERT D. MCKELVEY, Col, USAF  
Chief, Aeromechanics Division  
Air Force Flight Dynamics Laboratory



DANIEL M. PAROBK  
Tech Mgr, Experimental Engineer-  
ing Branch

Copies of this report should not be returned unless return is required by security considerations, contractual obligations, or notice on a specific document.

UNCLASSIFIED

SECURITY CLASSIFICATION OF THIS PAGE (When Data Entered)

REPORT DOCUMENTATION PAGE		READ INSTRUCTIONS BEFORE COMPLETING FORM
1. REPORT NUMBER AFDL-TR-78-82	2. GOVT ACCESSION NO.	3. RECIPIENT'S CATALOG NUMBER
4. TITLE (and Subtitle) RELATIVE TRANSITION PROBABILITY AND PRESSURE BROADENING PARAMETERS OF COPPER ATOMIC LINES		5. TYPE OF REPORT & PERIOD COVERED Final Technical April 15, 1975-August 31, 1977
7. AUTHOR(s) D. W. Boyer, W. H. Wurster, A. L. Russo C. E. Treanor		6. PERFORMING ORG. REPORT NUMBER WB-5726-A-3
9. PERFORMING ORGANIZATION NAME AND ADDRESS Calspan Corporation PO Box 235 Buffalo, New York 14221		8. CONTRACT OR GRANT NUMBER(s) F33615-75-C-3082
11. CONTROLLING OFFICE NAME AND ADDRESS Air Force Flight Dynamics Laboratory (FXN) Wright-Patterson AFB, Ohio 45433		10. PROGRAM ELEMENT, PROJECT, TASK AREA & WORK UNIT NUMBERS 1426-01-39 1781
14. MONITORING AGENCY NAME & ADDRESS (if different from Controlling Office)		12. REPORT DATE July 1978
		13. NUMBER OF PAGES 71
16. DISTRIBUTION STATEMENT (of this Report) Approved for public release; distribution unlimited.		15. SECURITY CLASS. (of this report) Unclassified
17. DISTRIBUTION STATEMENT (of the abstract entered in Block 20, if different from Report)		15a. DECLASSIFICATION/DOWNGRADING SCHEDULE
18. SUPPLEMENTARY NOTES Final rept. 15 Apr 75-31 Aug 77,		14. CALSPAN-WB-5726-A-3
19. KEY WORDS (Continue on reverse side if necessary and identify by block number) Cooper Lines Radiometer Line Shift Shock Tube Line Spectra Scanning Spectrometer Line Widths Transition Probability Pressure Broadening		
20. ABSTRACT (Continue on reverse side if necessary and identify by block number) The measured relative intensity ratios for the 5153 and 5106 angstroms copper atomic lines have been performed under optical thin conditions in argon as well as under non-thin conditions in molecular nitrogen and air. These measurements are shown to be in reasonably close accord with the results of Kock and Richter. The observed ratio of line width to line shift was found to be in reasonable accord with Lindholm's theoretical value for van der Waals' forces and in agreement with the ratio measured by Ovechkin and Sandrigailo for the 5106 angstroms copper line in collisions with molecular nitrogen.		

DD FORM 1 JAN 73 1473

EDITION OF 1 NOV 65 IS OBSOLETE

UNCLASSIFIED

SECURITY CLASSIFICATION OF THIS PAGE (When Data Entered)

407 727

set

## FOREWORD

This work was sponsored by the Air Force Flight Dynamics Laboratory, Air Force Systems Command, Wright-Patterson Air Force Base, Ohio, under Contract F33615-75-C-3082 and was performed by Calspan Corporation between April 1975 and October 1977.

The program initiator and technical monitor at AFFDL, up until September 1976, was Mr. Jon B. Bader. Subsequently, the program monitor responsibilities were assumed first by Dr. Robert F. Carpenter and then by Mr. Hsue-Fu Lee. The developments reported were carried out under Project 1426, "Experimental Simulation of Flight Mechanics," Task 142601, "Diagnostic, Instrumentation and Similitude Technology," and Work Unit 14260139, "Transition Probability and Pressure Broadening Parameters of Copper Atomic Lines".

The motivation for the present work was in the further development of a spectroscopic diagnostic technique for the measurement of blunt-body stagnation temperatures, employing the trace copper contamination present in the flows emerging from high-pressure arc facilities. Particular application of the diagnostic technique was proposed for the AFFDL ReEntry Nose Tip (RENT) Facility.

The authors gratefully acknowledge the major efforts performed by Mr. Robert E. Phibbs of Calspan Corporation in the performance of the laboratory measurements.

ACCESSION for	
NTIS	White Section <input checked="" type="checkbox"/>
DDC	Blue Section <input type="checkbox"/>
UNANNOUNCED	
JUSTIFICATION	
BY	
DISTRIBUTION/AVAILABILITY CODES	
Dist	Special

# TABLE OF CONTENTS

<u>Section</u>		<u>Page</u>
I	INTRODUCTION . . . . .	1
II	SHOCK TUBE AND AEROSOL-GENERATING SYSTEM . . . . .	3
	2.1 SHOCK TUBE. . . . .	3
	2.2 GENERATION OF COPPER AEROSOL AND SEEDING OF THE CARRIER TEST GAS. . . . .	5
III	RELATIVE TRANSITION-PROBABILITY MEASUREMENTS . . . . .	8
	3.1 OPACITY MONITOR . . . . .	8
	3.2 RELATIVE TRANSITION PROBABILITY MEASUREMENT SYSTEM. .	9
	3.3 MEASUREMENTS OF RELATIVE TRANSITION PROBABILITIES . .	9
IV	PRESSURE-BROADENED LINE WIDTH MEASUREMENTS . . . . .	12
	4.1 SCANNING SPECTROMETER . . . . .	12
	4.2 LINE-WIDTH MEASUREMENTS . . . . .	14
V	EXPERIMENTAL RESULTS AND DISCUSSION. . . . .	17
	5.1 THEORY USED FOR DATA REDUCTION. . . . .	17
	5.1.1 Intensity of Line Radiation, and Relative Intensities in the Thin-Line Limit . . . . .	17
	5.1.2 Effect of Doppler Broadening . . . . .	20
	5.1.3 Effect of Stark Broadening . . . . .	21
	5.1.4 Effect of Collision Broadening . . . . .	21
	5.1.5 Line Shift . . . . .	23
	5.1.6 Thick-Gas Effects for Collision-Broadened Lines; Intensity Ratios. . . . .	25
	5.1.7 Effects of Finite Slit-Width on Measured Line Width . . . . .	26
	5.2 RELATIVE TRANSITION PROBABILITY OF THE 5106Å AND 5153Å COPPER LINES. . . . .	27
	5.3 LINE WIDTH MEASUREMENTS . . . . .	34
	5.3.1 N <sub>2</sub> As Carrier Gas. . . . .	36
	5.3.2 Air As Carrier Gas . . . . .	46
VI	CONCLUSIONS AND RECOMMENDATIONS. . . . .	57
	6.1 CONCLUSIONS . . . . .	57
	6.2 RECOMMENDATIONS . . . . .	59
	REFERENCES . . . . .	60

# LIST OF FIGURES

<u>Figure</u>		<u>Page</u>
1	Schematic of Shock Tube Configuration . . . . .	4
2	Schematic of the Scanning Mirror Arrangement . . . . .	13
3	Third-Order Spectrum of Copper Atomic Lines. (Hollow-Cathode Copper Lamp Source) . . . . .	16
4	Relevant Energy Levels in Copper. . . . .	19
5	Ratio of Slit Function Half Width at Half Feight to Line Half Width at Half Height - Observed vs. True (Collision-Broadened Line, Gaussian Slit Function) . . . . .	28
6	Typical Traces from the Opacity Monitor Viewing the 5106A Atomic Copper Line . . . . .	29
7	Output of Transition Probability Radiometers. Equilibrium Gas Temperature = 4030°K . . . . .	30
8	Ratio, R, of Intensity of 5153A to 5106A Lines of Atomic Copper . . . . .	33
9	Comparison of Time-Integrated Spectra from Shock Tube and Hollow-Cathode Copper Source. N <sub>2</sub> Carrier Gas . . . . .	35
10	Spectral Scans of the 5106A Copper Atomic Line. N <sub>2</sub> as Cu-Aerosol Carrier Gas . . . . .	37
11	Output of 5106A and 5153A Line Two-Channel Radiometer. N <sub>2</sub> as Cu-Aerosol Carrier Gas . . . . .	38
12	Output of the Opacity Monitor Viewing the 5106A Cu Line. N <sub>2</sub> Carrier Gas . . . . .	41
13	Spectral Scans of the 5106A Copper Atomic Line. Air as the Cu-Aerosol Carrier Gas . . . . .	47
14	Output of 5106A and 5154A Line Two-Channel Radiometer. Air as Cu-Aerosol Carrier Gas . . . . .	48
15	Spectral Scan and Radiometer Response from Reflected Shock Region in Pure Air . . . . .	49
16	Spectral Scans of Reflected-Shock Region in Air with and Without Copper Aerosol . . . . .	51
17	Spectral Scan of Tungsten Source . . . . .	53

# LIST OF TABLES

<u>Table</u>		<u>Page</u>
1	Constants for $\lambda$ 5106.54 and 5153.24 Copper Lines . . . . .	18
2	Slit Width Correction for Measured $\lambda$ 5106 Line Half Widths . .	40
3	Estimation of Effect of Optical Thickness . . . . .	43

# LIST OF SYMBOLS

$A$	Transition probability for spontaneous emission
$c$	Speed of light
$C_v$	van der Waal's interaction constant
$E$	Energy of electronic level
$g$	Degeneracy of electronic level
$h$	Planck's constant
$k$	Boltzmann constant
$k(\lambda)$	Spectral absorption coefficient
$l$	Path length
$L$	Mean freepath
$m$	Mass of molecule
$M$	Molecular weight
$n$	Number density
$n_0$	Loschmidt number
$N_\lambda$	Spectral line radiance
$N_\lambda^0$	Black body spectral radiance
$P$	Pressure
$Q$	Electronic partition function
$R$	Distance to perturbing particle
$R$	Universal gas constant
$S$	Line strength

# LIST OF SYMBOLS (Cont.)

$T$	Temperature
$u$	Optical depth
$v$	Average molecular velocity
$\Delta V$	Potential energy of collision interaction
$W$	Line equivalent width
$X$	Optical thickness parameter = $0.25 S u / \delta_c$
$\gamma$	Half width at half height of spectral line profile
$\delta \gamma$	Half width at half height of instrument slit function
$\lambda$	Wavelength
$\lambda_0$	Wavelength at line center
$\rho_i$	Optical collision diameter for species $i$
$\Delta_c$	Shift of the line center for van der Waal's interaction

## SUBSCRIPTS

$c$	Collision broadened
$d$	Doppler broadened
$i$	Species $i$
$l$	Lower level of electronic transition
$o$	Standard reference conditions
$s$	Stark broadened
$u$	Upper level of electronic transition.

## SUMMARY

Relative transition probability measurements for the  $5153\text{\AA}$  and  $5106\text{\AA}$  copper atomic lines have been performed under optically thin conditions in argon, at a temperature of  $4,000^\circ\text{K}$ . The measured relative intensity ratios,  $R$ , for the two copper lines are shown to be in reasonably close accord with the results of Kock and Richter. Relative copper line intensity measurements were also obtained under non-thin conditions, as complementary data to  $5106\text{\AA}$  copper line-broadening measurements performed in  $\text{N}_2$  and air. The measurements in  $\text{N}_2$ , at a temperature near  $5,900^\circ\text{K}$ , were found to yield  $R$  values which were in close proximity to the curve defined by the optically thin results. However, considerations of optical thickness effects on these data have shown the results to be inconsistent with the predicted effects of self absorption, based on separate opacity measurements. It is concluded that the opacity measurements are in error, and the gas is not as thick as the opacity measurements indicate. Relative intensity measurements were also obtained in air at a temperature near  $5,000^\circ\text{K}$ . These data were super-imposed upon a high level of background radiation within the radiometer filter band-passes. On the basis of supplementary measurements performed in pure air a correction for the background radiation could be investigated. The corrected relative intensity ratio for the copper lines was then also found to exhibit close correlation with the measured  $R$  values at  $4,000^\circ\text{K}$  and  $5,900^\circ\text{K}$ . The effect of pressure broadening on the  $5106\text{\AA}$  copper line was investigated in the shock tube experiments using both  $\text{N}_2$  and air as Cu-aerosol carrier gases. Spectral scans of the  $5106\text{\AA}$  Cu line in  $\text{N}_2$  exhibited an increase in the measured line width which was consistent with the two-fold increase in total gas pressure. The measured half width at half height for the  $5106\text{\AA}$  Cu line,

reduced to standard temperature and pressure conditions, was 0.021Å. The corresponding optical collision diameter was 5.7<sup>o</sup>Å, which is close to the value reported by Ovechkin and Sandrigailo. Similar spectral scan measurements of the 5106<sup>o</sup>Å Cu line in air were comprised by a high level of underlying continuum-like radiation within the wavelength intervals of interest. This background radiation was shown to originate from the heated air carrier gas. Corrections for background radiation were made to the 5106<sup>o</sup>Å Cu line scan data in Cu-seeded air at 90.3 atm total pressure on the basis of spectral scan measurements performed in air without copper. The corrected line profile was used to provide a reasonable estimate for the line half width, at standard temperature and pressure in air, which indicated no apparent effect due to the presence of O<sub>2</sub> on the 5106<sup>o</sup>Å line width. The 5106<sup>o</sup>Å line center was observed to be shifted to longer wavelength with increase in N<sub>2</sub> gas pressure. The observed ratio of line full width at half height to line center shift was found to be in reasonable accord with Lindholm's theoretical value for van der Waals' forces and in agreement with the ratio measured by Ovechkin and Sandrigailo for the 5106<sup>o</sup>Å copper line in collisions with N<sub>2</sub> molecules.

## SECTION I

### INTRODUCTION

In high-pressure arc facilities the test air is heated by a high-energy electric discharge between copper electrodes. Typically, the high-temperature arc conditions and electrode erosion introduce unknown amounts of atomic copper into the air flow. It is possible, however, that under favorable conditions the presence of the atomic copper contaminant can be used as a thermometric species in spectroscopic diagnostics of the arc-heated air.

Copper possesses a number of atomic lines in the visible spectral region (5106Å, 5153Å, 5218Å, 5220Å, 5700Å, 5728Å): the ratio of the relative radiance of selected pairs of these lines (5105 and 5153, for example) can be used to infer the electronic temperature of the copper. For this spectral region (5106 and 5153Å) the radiance of these atomic copper lines varies approximately as the third and sixth power of the temperature at temperatures of 10,000 and 5000 K respectively. Because of the strong temperature dependence the measurement of the relative line radiances of the copper atom offers a means for accurately measuring the temperature of the air environment under conditions of thermal equilibrium.

The implementation of such a diagnostic is predicated, of course, upon an accurate knowledge of the spectroscopic parameters of atomic copper. In particular, it is required that the relative transition probabilities of the 5106 and 5153Å lines of atomic copper and the line shapes under typical arc-facility conditions of pressure broadening and Stark broadening be known. The general objective of this research program was to conduct a program of laboratory measurements to provide some of these basic data.

A pure copper aerosol was generated in suspension in air,  $N_2$  and argon as carrier test gases, and compressed and heated to controlled and known thermodynamic conditions in a shock tube. The primary data consisted of relative line radiance measurements and line-width measurements under conditions where the line width was determined by pressure broadening.

The diagnostic instrumentation, measurement techniques, theoretical considerations and the experimental results are discussed herein.

## SECTION II

### SHOCK TUBE AND AEROSOL-GENERATING SYSTEM

#### 2.1 SHOCK TUBE

The shock tube has found wide application in the processing of gases to known high values of equilibrium temperature and pressure for diagnostic observation and measurement. In particular, the shock tube employed in the present studies was specifically designed for radiation measurements from shock-heated gases. Such measurements have encompassed the wavelength region from the vacuum ultraviolet (800Å) to the short wavelength infrared ( $5\text{ }\mu\text{m}$ ), temperatures from  $2,000^{\circ}\text{K}$  to  $13,000^{\circ}\text{K}$ , employing a wide variety of pure test gases and specific gas mixtures.

The shock tube employed in the present studies is shown schematically in Figure 1. It consists of a 30-foot length of 3-inch diameter driven tube and a 5-foot length of 4-inch diameter driver tube. Depending upon the incident shock Mach number requirements for processing of the driven-tube test gas, the driver gas may be selected as either room-temperature  $\text{H}_2$ , He or  $\text{N}_2$ . Both helium and hydrogen were employed as driver gases in the present experiments.

Prior to each experiment, the driven section is routinely pumped to the order of  $10^{-2}\text{ }\mu\text{Hg}$  (ionization gauge readout) by means of a liquid-nitrogen trapped diffusion pump system. The driven tube is then loaded with the test gas (carrier gas + Cu aerosol in the present case) to a prescribed initial pressure. The driver tube is then pressurized to provide the driver/driven gas pressure ratio required to generate the desired incident shock velocity through the test gas in the driven tube. Shock speed reproducibility is insured through use of the double-diaphragm technique, which utilizes two mild-steel scribed diaphragms for each test. As the incident shock wave traversed the last 12 feet of driven tube, its passage was detected by means of flush-mounted heat transfer gauges installed in the tube wall (Figure 1). The time intervals between shock arrival at these precisely-located stations

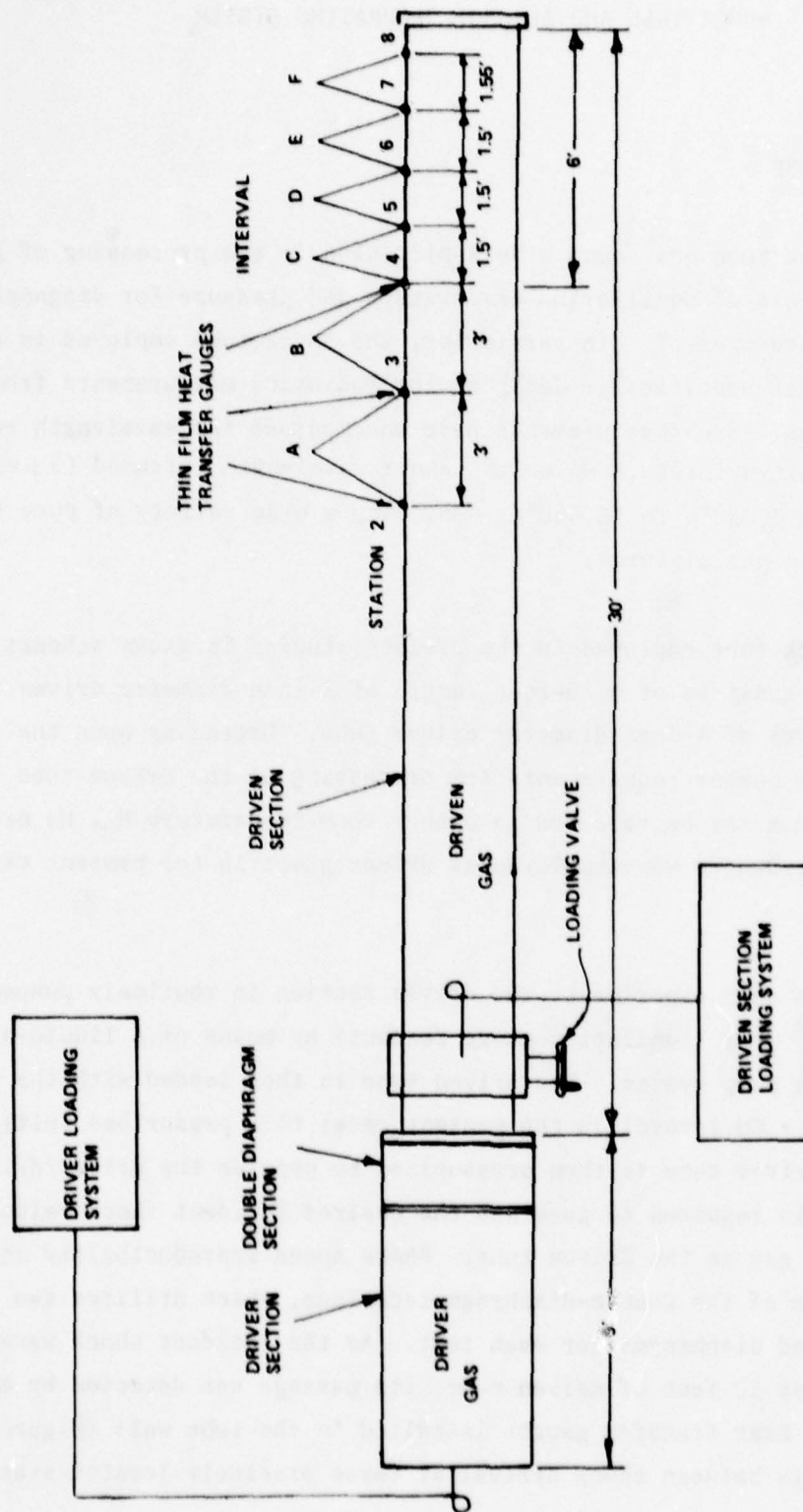


Figure 1. SCHEMATIC OF SHOCK TUBE CONFIGURATION

was recorded by megacycle interval counters to provide an accurate measurement of wave speed as the shock approached the end wall. Excellent repeatability ( $\sim 1\%$ ) in measured shock speed was routinely achieved in repeat experiments.

Upon shock reflection from the end wall, the gas behind the incident shock is further compressed to the higher temperature and pressure conditions desired. The measured incident shock speed, together with initial test gas conditions permit the calculation of the reflected-shock test gas conditions to be computed with a reliability which depends on the accuracy of available thermo-chemical data. Reflected shock calculations performed with and without the presence of the copper indicated a negligible effect on the state thermodynamic parameters ( $< 0.5\%$ ) due to the copper.

For a given shock speed, the incident and reflected test times are determined by both the tube length and operating pressure of the experiment. As noted, the test section length for the radiation shock tube is 30 feet, which gives rise to test times more than sufficient to include passage of the shock front, finite rate chemistry, excitation and nonequilibrium phenomena and steady-state equilibrium condition as well as allowing synchronization of various diagnostic techniques. As in any shock-tube facility, however, the experimentally attained test time decreases as the initial pressure decreases and wall boundary layers thicken. Previous experimental data indicate that only about 35% of the calculated test time is achieved for initial pressures of 1 torr or less. However, such low pressure conditions were not pertinent in the present experiments and the measured test times (from 150 to 300  $\mu$ secs) were quite adequate for the diagnostic measurements to be discussed.

## 2.2 GENERATION OF COPPER AEROSOL AND SEEDING OF THE CARRIER TEST GAS

Several different methods have been employed to produce metal-bearing gases for use in shock tube research. In the present experiments, the exploding-wire aerosol technique was used to introduce the copper into the shock tube.

This technique has been used most successfully in previous studies at Calspan using aluminum,<sup>1</sup> platinum<sup>2</sup> and uranium<sup>3</sup> aerosols.

The method consists of exploding a short length of pure copper wire in a 4-in. dia. by 4-in. long cylindrical (aerosol) chamber attached to the end wall of the shock tube test section. The aerosol chamber volume is about 1/50 the volume of the shock tube test section and incorporates a pair of copper jaw electrodes to clamp the 0.005 in or 0.010 in diameter copper wire with capability for installation of variable lengths of wire up to 1 inch long. The wire is exploded by means of a capacitor discharge ( $\sim 2200$  joules), thereby producing a metallic copper smoke or aerosol in the small chamber.

In practice, the carrier test gas (Ar, N<sub>2</sub> or air) is introduced into the initially evacuated aerosol chamber to a pressure of 1 atm, the wire is exploded, and the aerosol chamber pressure is then further increased to a prescribed value by the introduction of additional carrier gas. A valve is then opened to admit the test gas + Cu aerosol suspension into the evacuated driven section of the shock tube. The prescribed aerosol chamber pressure prior to volume communication with the shock tube is such that the introduction of the test gas + aerosol produces the desired initial driven-tube pressure in the shock tube. The aerosol chamber is then isolated by closing the communicating valve and the shock tube driver is pressurized for the execution of the run.

The exploding wire technique produces an aerosol with submicron-size particles which have been shown (e.g., Ref. 2) to vaporize readily in times which are short compared with the reflected shock test-time interval. No particulate settling in the shock tube is involved at the pressures and time intervals pertinent in these experiments. The total amount of copper present

1. Wurster, W.H. Shock-Tube Spectroscopy of Ablative Species, Proc. Sixth International Shock Tube Symposium, Freiburg, Germany, April 1967, Physics of Fluids Supplement, 12, I-92, May 1969.
2. Falk, T.J. Evaporation of Submicron Platinum Particles in a Shock Tube, J. Chem. Phys., 48, 3305, April 1968.
3. Wurster, W.H. Uranium-Oxygen Radiation Studies, Final Report, DNA 3398F, Calspan Corporation 1974.

in the carrier gas cannot be determined directly. Previous experience with this technique<sup>3</sup> has shown that a fraction,  $\leq 5\%$ , of the total copper vaporized can be expected in the high-temperature test gas.

The relative transition probability measurements employed a 2 mm length of 0.005 in. diameter Cu wire. At the reflected-shock conditions for these experiments,  $T \sim 4000^\circ\text{K}$ ,  $P \sim 32$  atm., wherein the carrier gas number density was about  $6 \times 10^{19} \text{ cm}^{-3}$  a Cu-atom number density of about  $10^{13} \text{ cm}^{-3}$  would be expected. For the line-width measurements, a 0.9 in. length of 0.010 in. diameter Cu wire was used. In this case, if all the Cu that is vaporized were contained in the final test gas, the Cu loading would correspond to about 0.1 percent mole fraction at the reflected shock test conditions. However, at the total number densities of about  $5 \times 10^{19}$  to  $10^{20} \text{ cm}^{-3}$  involved in these tests, typical Cu-atom number densities of about  $10^{15} \text{ cm}^{-3}$  would be expected.

### SECTION III

#### RELATIVE TRANSITION PROBABILITY MEASUREMENTS

The determination of the relative transition probabilities for the 5106Å and 5153Å Cu lines was obtained from measurements of the relative line radiances from the shock-heated test gas. A principal requirement for the measurements of the transition probability ratio, however, is the existence of optically thin line radiation conditions. An opacity-monitor instrument was therefore designed and implemented for monitoring the optically thin condition during the course of the relative transition probability measurements.

#### 3.1 OPACITY MONITOR

The line opacity monitoring system was a twin-beam system with which the 5106Å Cu line radiance was monitored for a single and double-pass transit of the shock tube diameter. The system comprised two photodiode detectors fitted with appropriate field stops. The field stops are positioned and focussed by means of a simple lens to define identical and largely overlapping volumes at the same axial shock-tube location. The opposite wall of the shock tube is fitted with a window, half of which is rendered almost completely absorbing while the other half is almost completely reflecting. One of the photodiodes viewed the absorbing wall while the other viewed the reflecting wall. For an optically thin gas, the ratio of the output signals has been calculated to be about 1.85. The opacity monitor viewed the radiation from the 5106Å line by using a narrow-bandpass (12Å) interference filter centered at 5108Å. Calibration of this system involved the adjustment for identical overall system response for both channels. The calibration was performed in a separate optical-bench experimental setup<sup>4</sup> wherein the opacity monitor detector systems were illuminated by means of a tungsten ribbon-filament lamp. A focusing lens and a beam chopper were also incorporated into the optical path, the former being installed on a small micrometer traverse platform. The tungsten source was thereby traversed across each detector field of view and the overall system gains between the two channels were carefully balanced by means of a variable potentiometer in one of the detector-amplifier circuits.

4. Russo, A.L. and Wurster, W.H., Transition Probability and Pressure Broadening Parameters of Copper Atomic Lines, Interim Technical Report, Calspan Report No. WB-5726-A-2, January 1976.

### 3.2 RELATIVE TRANSITION PROBABILITY MEASUREMENT SYSTEM

The measurement system for the relative transition probabilities of the 5106 $\text{\AA}$  and 5153 $\text{\AA}$  lines of atomic copper comprised a split-beam two-channel filter radiometer system. The radiation from the test gas at known thermodynamic conditions was imaged by a lens onto a spectrometer slit mechanism. The throughput radiation was divided (approximately 30% each) by a transmission/reflection beamsplitter and passed through individual narrow bandpass ( $\sim 12\text{\AA}$ ) filters onto photomultipliers. This approach provided greater overall optical throughput than could be achieved with a spectrograph system.

Accurate analysis of the test data required the precise determination of the transmission of the optical filters at the two copper lines of interest (5106 $\text{\AA}$  and 5153 $\text{\AA}$ ). These calibrations were obtained using a Perkin-Elmer Model 460 Atomic Absorption Spectrophotometer and a Perkin-Elmer hollow-cathode copper lamp. The calibration was precise and additional considerations of slit functions, astigmatism or coma associated with spectrographs were not required.

### 3.3 MEASUREMENTS OF RELATIVE TRANSITION PROBABILITIES

Initial calibration experiments were performed to establish suitable shock tube operating conditions for the relative transition probability measurements and to define the sensitivity and signal to noise performance of the diagnostics.

The relative transition-probability measurements were performed using argon as the Cu-aerosol carrier gas. The initial tests included the selection of suitable driver-to-driven gas pressure ratios required to produce test gas temperatures in the range 3500 - 4500 $^{\circ}\text{K}$ . In addition, several test runs were made to confirm the reproducibility of a given test condition. Two series of tests indicated wave speed reproducibility to better than 1% which corresponds to temperature reproducibility of the test gas to better than about 100 $^{\circ}\text{K}$  for the temperature range of interest. Furthermore, several tests were

next conducted with and without the addition of copper aerosol to the test gas. The results of these tests confirmed that the observed signals were directly attributable to the presence of the copper. Moreover, these data showed a good signal-to-noise ratio, and a uniform radiation history over the test interval of about 300  $\mu$ secs from reflected-shock arrival.

During the initial data acquisition experiments, occasional discrepancies were observed in the temporal profiles of the radiance of the 5106Å and 5153Å atomic copper lines from the transition probability diagnostics. Because a differential background could give rise to such an effect, it was considered mandatory to measure the background radiation between the two copper lines of interest.

In view of the unavailability of suitable narrow-bandpass filters for this purpose, the optical system was modified so as to incorporate a 3/4-meter Jarrel Ash spectrometer into the optical diagnostics. This instrument was equipped with a 600 lines/mm grating blazed for 5000Å resulting in a linear dispersion of 20Å/mm in first order.

Approximately 50% of the radiation from the shock-heated gas used for the transition probability measurements was deflected by a beamsplitter and suitably imaged onto the entrance slit (50  $\mu$ m) of the spectrometer. A mask, with a slit 1 mm x 10 mm, was located at the exit plane of the spectrometer and the radiation passing through this slit was monitored by a Dumont K2190 photomultiplier. The hollow-cathode copper lamp was used, first to identify the copper atomic lines, and secondly, to set the grating of the spectrometer so that the exit slit and photomultiplier could view either the 5106Å or the 5153Å copper lines, or any background radiation centered at 5130Å.

Several runs were performed to provide a relative calibration of the spectrometer system with respect to the radiometer systems used for the transition probability measurements. The output of the spectrometer system was compared with the radiometers by adjusting the grating to view the 5106Å and 5153Å lines in sequential runs. Finally, the grating was adjusted to

view any background radiation between the lines in the region centered at 5130Å. The results of these complementary experiments indicated that the background radiation contributed, typically, about 20% to the radiation measured for the 5153Å line, and about 1% to that for the 5106Å line.

The final relative transition probability measurements (Ar/Cu) were performed at reflected-shock gas temperatures ranging from 4000 to 4070°K, at a pressure of about 32 atm. The measured relative intensities of the 5106Å and 5153Å copper lines were corrected for the effects of background radiation. Furthermore, the ratio of the intensities measured by the opacity monitor system were about 2 to 1 for the reflecting and nonreflecting walls respectively, indicating optically thin conditions for the transition probability line-radiation measurements. These results are described in Section 5.2. Similar two-channel radiometer data were also obtained, under non-thin conditions, during the line-width measurements. These data are discussed in Section 5.3.

SECTION IV  
PRESSURE-BROADENED LINE WIDTH MEASUREMENTS

4.1 SCANNING SPECTROMETER

The primary requirement for the line-broadening measurements is the achievement of the spectral line scan within the available shock tube test time, and its routine and reliable synchronization with shock tube operation.

The basic diagnostic instrument for the line-width measurements was a 3/4-meter Jarell Ash spectrometer whose post-focal plane optics incorporated a specially designed scanning mirror arrangement which swept a magnified image of the spectral line across a narrow scan slit located in front of a photo-multiplier detector.

The spectrometer was equipped with a 1200 lines/mm grating blazed for 7500Å with the Cu lines observed in third order. The measured linear dispersion at the spectrometer focal plane was 3Å/mm in third order. The spectral line at the spectrometer focal plane was imaged onto the scan slit by means of the optical scan system. The scan optics afforded a two-fold magnification of the spectrometer slit image and comprised a lens and the impulsively driven scan mirror.

The scan mirror arrangement is shown schematically in Figure 2. The 14 x 19 mm front-surface mirror is cemented (epoxy) onto a shaft whose ends are mounted in jeweller ball bearings to ensure that the mirror spins freely. The mirror is initially rotated so that its back surface rests against a hairpin-shaped thruster wire which is connected to a storage capacitor. An ignitron circuit initiates the capacitor discharge, thereby ohmically heating the thruster wire which elongates and effects an impulsive rotation of the scan mirror. Synchronization with shock tube operation is precisely controlled by means of an ignitron-trigger signal obtained from one of the shock velocity measuring stations on the shock tube (Fig. 1), and a variable time delay unit.

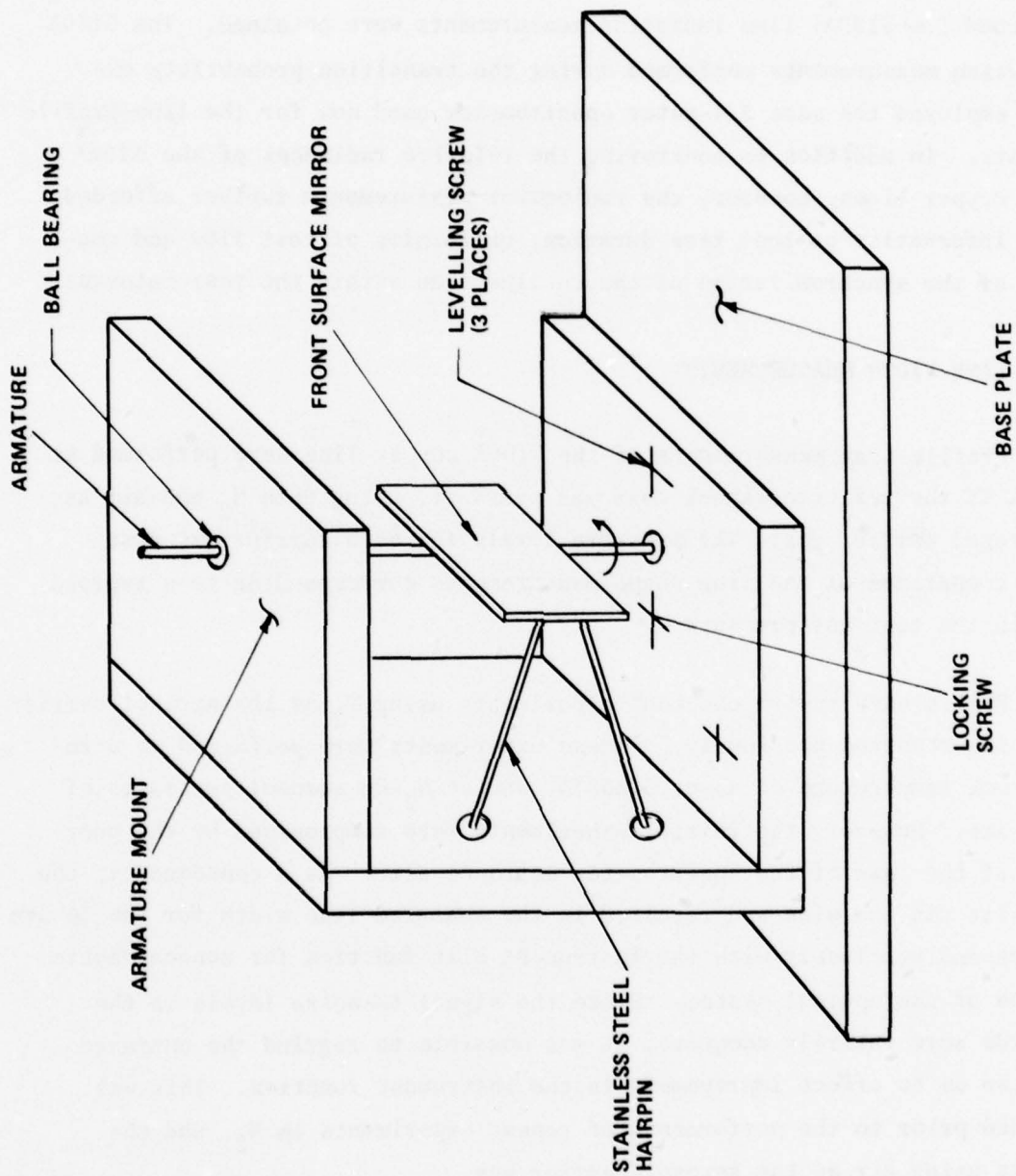


Figure 2. SCHEMATIC OF THE SCANNING MIRROR ARRANGEMENT

The opacity monitor and transition probability radiometer diagnostics were also employed during the line-width experiments. However, the 5106Å and 5153Å line radiometric measurements were more qualitative in this case in that no background ( $\sim 5130\text{Å}$ ) line radiation measurements were obtained. The 5130Å line radiation measurements performed during the transition probability experiments employed the same 3/4-meter spectrometer used now for the line-profile measurements. In addition to monitoring the relative radiances of the 5106Å and 5153Å copper lines, however, the radiometer measurements further afforded important information on test time duration, uniformity of test flow and confirmation of the synchronization of the Cu line scan within the test interval.

#### 4.2 LINE-WIDTH MEASUREMENTS

Profile-scan measurements of the 5106Å copper line were performed at two values of the reflected-shock test gas pressure, using both  $\text{N}_2$  and air as the Cu-aerosol carrier gas. The pressure levels for each carrier gas case permitted comparison of the line shape measurements corresponding to a twofold increase in the test gas pressure.

Preliminary system checkout experiments using  $\text{N}_2$  as the aerosol carrier gas have been reported previously.<sup>5</sup> These experiments were performed at a reflected-shock temperature of about 5,800°K, and at  $\text{N}_2$ -Cu aerosol pressures of 36 and 70 atm. However, the initial experiments were compromised by the poor condition of the jaws of the spectrometer entrance slit. As a consequence, the entrance slit was too wide and resulted in the measured line width for the 36 atm case corresponding closely with the instrument slit function for monochromatic irradiation of the optical system. Since the signal-to-noise levels in the scan records were entirely adequate, it was possible to regrind the entrance slit jaws so as to effect improvement in the instrument function. This was accomplished prior to the performance of repeat experiments in  $\text{N}_2$ , and the experiments using air as the aerosol-carrier gas.

5. Boyer, D.W., Russo, A.L. and Wurster, W.H., Transition Probability and Pressure Broadening Parameters of Copper Atomic Lines, Interim Progress Report, 1 January 1977 - 15 February 1977.

A hollow-cathode copper lamp was used to adjust the spectrometer grating to view the copper lines in the spectral region of interest in third order. A narrow-band 5106Å filter was then employed to identify the 5106Å Cu line and to permit its suitable positioning in the spectrometer focal plane. A Polaroid photograph of the Cu atomic lines with and without the 5106Å filter in the optical system is shown in Figure 3. As noted, the measured linear dispersion at the spectrometer focal plane was 3Å/mm, corresponding to 1.5Å/mm at the scan slit.

The spectrometer entrance slit width was selected on the basis of initial line-scan measurements of a mercury line. The spectrometer entrance slit was illuminated with a mercury "Penray" lamp source and spectral scans of the 5461Å Hg green line were recorded as a function of entrance slit width. The half-height widths ( $2Y$ ) of the Hg line scan profiles were plotted as a function of entrance slit width, and the slit width selected for the shock tube experiments was the minimum width for linear variation of slit width with half-height line width on the above plot. The entrance slit width used was 0.114 mm and the scan slit width was 0.038 mm. The corresponding instrument slit function measured for the spectrometer and scanner system was  $\delta\lambda = 0.17\text{Å}$ .

The test gas seeding with copper aerosol was accomplished in the manner described in Section 2.2. Following the explosion of the copper wire in the aerosol chamber in 1 atm pressure of carrier gas, the aerosol chamber pressure was increased with additional carrier gas to either 40 psig or 100 psig, prior to admitting the contents to the driven section of the shock tube. The same  $\text{H}_2$  driver-gas to driven-gas pressure ratio was employed throughout the line-width measurement tests.

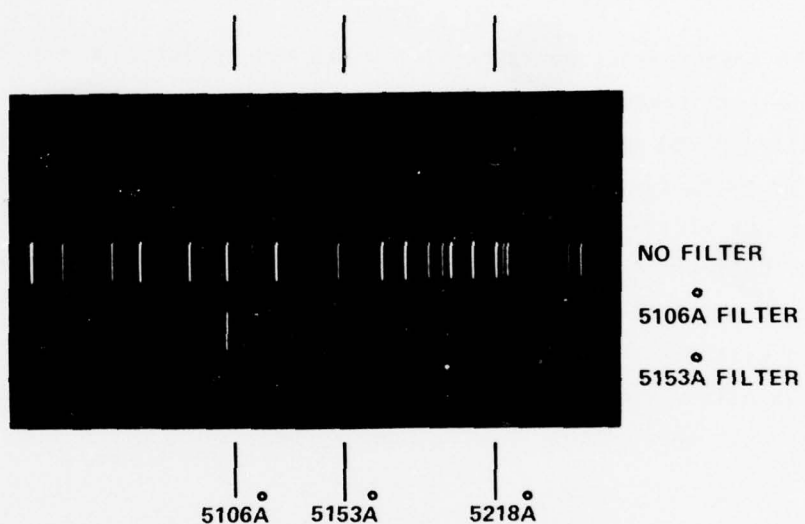
Scans of the 5106Å copper atomic line were recorded at the following reflected-shock test conditions:

With  $\text{N}_2$  as aerosol carrier gas,

$$\begin{aligned} T &= 5830^\circ\text{K}, \quad P = 35.7 \text{ atm}, \quad n \approx 4.5 \times 10^{19} \text{ cm}^{-3} \\ T &= 5960^\circ\text{K}, \quad P = 70.0 \text{ atm}, \quad n \approx 9 \times 10^{19} \end{aligned}$$

With air as aerosol carrier gas,

$$\begin{aligned} T &= 4975^\circ\text{K}, \quad P = 45.8 \text{ atm}, \quad n \approx 6.5 \times 10^{19} \\ T &= 4970^\circ\text{K}, \quad P = 90.3 \text{ atm}, \quad n \approx 1.3 \times 10^{20} \end{aligned}$$



MEASURED LINEAR DISPERSION = 3A/MM

Figure 3. THIRD-ORDER SPECTRUM OF COPPER ATOMIC LINES.  
(HOLLOW-CATHODE COPPER LAMP SOURCE)

## SECTION IV EXPERIMENTAL RESULTS AND DISCUSSION

### 5.1 THEORY USED FOR DATA REDUCTION

#### 5.1.1 Intensity of Line Radiation and Relative Intensities in the Thin-Line-Limit

For any volume of gas, the total radiation rate from the surface per unit area and per unit solid angle for a given spectral line is called the line radiance:

$$N_i = \int N_\lambda d\lambda \quad (1)$$

where  $N_\lambda$  = spectral line radiance =  $N_\lambda^0 (1 - e^{-k(\lambda)u})$ ,  $N_\lambda^0$  is the black-body spectral radiance, and  $k(\lambda)$  is the spectral absorption coefficient, whose half-width at half-height is  $\gamma \text{ \AA}$ .  $u$  is the optical path length,  $u = \frac{n_\lambda}{n_0} \ell$ , where  $n_\lambda$  is the number density of radiating atoms,  $n_0$  is the Loschmidt number ( $n_0 = 2.687 \times 10^{19} \text{ cm}^{-3}$ ) and  $\ell$  is the path length. Alternately expressed

$$N_i = N_\lambda^0 W_i \quad (2)$$

$$\text{where } W_i = \text{equivalent width of line} = \int (1 - e^{-k(\lambda)u}) d\lambda \quad (3)$$

The important parameters for describing the line radiance are the line strength  $S$

$$S = \int k(\lambda) d\lambda \quad (4)$$

and the optical path length  $u$ . The product  $Su$  is related to the number density of radiators ( $n_\lambda$ ), the energy of the lower state ( $E_1$ ), the degeneracy of the upper state ( $g_u$ ) and the lifetime for the transition ( $A$ ) by:

$$S u = 3.57 \times 10^{-7} \frac{n_\lambda}{n_0} g_u A \lambda^4 \frac{e^{-E_1/kT}}{Q(T)} \ell \quad (5)$$

With  $\ell$  in cm,  $\lambda$  in cm and  $A$  in  $\text{sec}^{-1}$ , this constant ( $\frac{n_0}{8\pi c} = 3.57 \times 10^7 \frac{\text{sec}}{\text{cm}^2}$ ) gives  $S_u$  in cm.  $Q(T)$  is the electronic partition function and  $T$  is the temperature ( $^{\circ}\text{K}$ ). For the two lines of interest in the present work, the energy level diagram is shown in Figure 4. The relevant constants are given in Table 1.

TABLE 1  
Constants for  $\lambda$  5105.54 and 5153.24 Copper Lines

$\lambda(\text{\AA})$	$E_\ell(\text{cm}^{-1})$	$\frac{E_\ell}{k}(^{\circ}\text{K})$	$g_u A (\text{sec}^{-1})$
5105.54	11202.565	16100	$0.079 \times 10^8$ [From 1970 review data of Ref. 6, as cited in Ref. 7]
5153.24	30535.302	43900	$2.45 \times 10^8$

Values of the partition function can easily be calculated from the relation

$$Q(\tau) = \sum g_i e^{-E_i/kT}$$

giving

$$Q(4000^{\circ}\text{K}) = 2.141$$

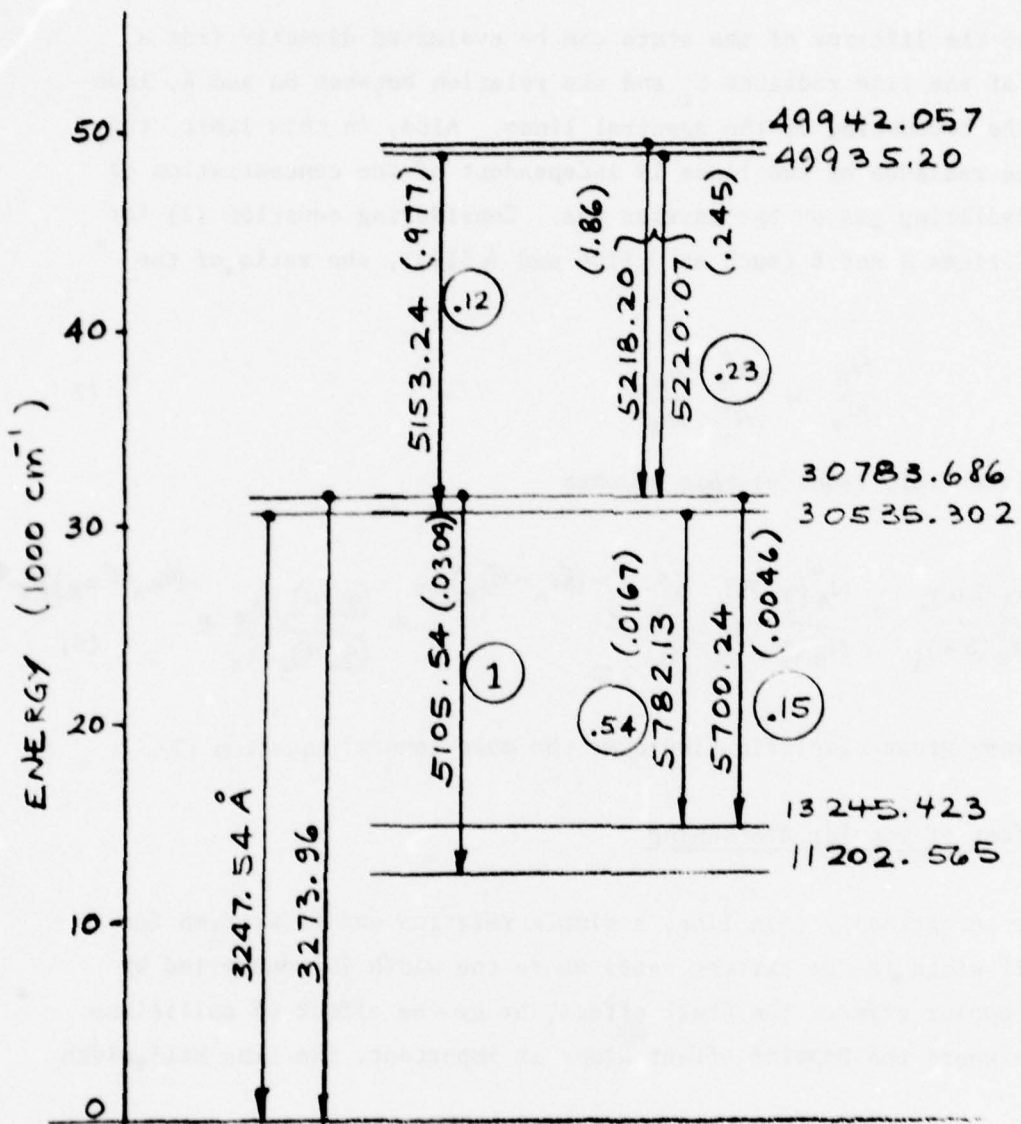
$$Q(6000^{\circ}\text{K}) = 2.577$$

#### Thin Gas Approximation

If the value of  $k(\lambda)u$  is small compared with unity, the expression for the effective width of the line becomes

$$W_i = \int \left[ 1 - (1 - k(\lambda)u + \frac{1}{2} k^2(\lambda)u^2 - \dots) \right] d\lambda \simeq \int k(\lambda)u d\lambda = Su \quad (6)$$

6. Corliss, C.H. A Review of Oscillator Strengths for Lines of CuI. Journal of Research-A. Physics and Chemistry, 74A, No. 6, 781, (1970).
7. Bader, Jon B., Time-Resolved Absolute Intensity Measurements of the 5106 Angstrom Copper Atomic Spectral Line in the AFFDL RENT Facility, AFFDL Technical Report TR-75-33, June 1975.



(gf) KOCK & RIKHTER

○ RELATIVE  
INTENSITIES  
(~5000°K)

Figure 4. RELEVANT ENERGY LEVELS IN COPPER

In this limit the lifetime of the state can be evaluated directly from a measurement of the line radiance  $N_i$  and the relation between  $S_u$  and  $A$ , independent of the broadening of the spectral lines. Also, in this limit, the ratios of the radiance of two lines is independent of the concentration of either the radiating gas or the carrier gas. Considering equation (2) for two spectral lines A and B (such as  $\lambda 5106$  and  $\lambda 5153$ ), the ratio of the radiance is

$$\frac{N_A}{N_B} = \frac{N_A^0}{N_B^0} \frac{W_A}{W_B} \quad (7)$$

In the thin-gas limit (eqn. 6) this becomes

$$\frac{N_A}{N_B} = \frac{N_A^0 (S_u)_A}{N_B^0 (S_u)_B} = \frac{N_A^0 (g_u A)_A}{N_B^0 (g_u A)_B} \frac{\lambda_A^+}{\lambda_B^+} e^{-(E_{lA} - E_{lB})/kT} = \frac{(g_u A)_A}{(g_u A)_B} \frac{\lambda_B}{\lambda_A} e^{-(E_{uA} - E_{uB})/kT} \quad (8)$$

which is a very great simplification over the more general equation (7).

### 5.1.2 Effect of Doppler Broadening

For an optically thin line, a simple relation can be written for the line half-width in the extreme cases where the width is controlled by either the Doppler effect, the Stark effect, or by the effect of collisions. For the case where the Doppler effect alone is important, the line half width is given by

$$\gamma_d = \frac{0.83 \lambda_0}{c} \sqrt{\frac{2RT}{M}} \quad (9)$$

where  $\gamma_d$  is half of the width of the line at half height,  $\lambda_0$  is the wavelength of the line center, and  $T$  is the temperature of the gas ( $^{\circ}\text{K}$ ).  $M$  is the molecular weight,  $R$  the gas constant ( $8.3 \times 10^7$  erg/mol $^{\circ}\text{K}$ ) and  $c$  the speed of light ( $3 \times 10^{10}$  cm/sec). Using  $M = 63.6$  for Cu and  $\lambda = 5125\text{\AA}$  (an average value for  $\lambda 5106$  and  $\lambda 5153$ ), this becomes

$$\gamma_d = 2.3 \times 10^{-4} \sqrt{T} \quad \text{\AA}$$

For the temperatures and pressures in the shock tube experiments ( $\sim 5,000^\circ\text{K}$ , 40-80 atm), the Doppler half width is much smaller than the observed half width (0.016\AA compared with  $\sim 0.25\text{\AA}$ ). Thus the effect of Doppler broadening can safely be ignored in the analysis of the data.

### 5.1.3 Effect of Stark Broadening

The Stark broadening of the spectral lines is caused by collisions with free electrons, and thus the semi half width is proportional to the number density of electrons

$$\gamma_s = C_s \frac{n_e}{n_o}$$

where the broadening constant  $C_s$  typically varies from 1 to 4 \AA/10<sup>17</sup> cm<sup>-3</sup>. Thus for electron densities less than  $\sim 10^{15}$  cm<sup>-3</sup> broadening would be small compared with the observed half width of  $\sim 0.25\text{\AA}$ . For the test conditions considered here, the electron densities from both the carrier gas and the Cu vapor are below this level. (In the extreme case, air at 4970°K and 90 atm pressure, nitric oxide ionizes easily, and the number density of electrons is  $1.2 \times 10^{15}$  elec/cm<sup>3</sup>). From these considerations Stark broadening effects can be ignored in reducing the present data.

### 5.1.4 Effect of Collision Broadening

A relation for the collision broadened semi-half width of an optically thin spectral line can be written

$$\gamma_c = \gamma_{oi} \frac{n_i}{n_o} \sqrt{\frac{T}{T_o}} = \gamma_{oi} \frac{P_i}{P_o} \sqrt{\frac{T}{T_o}} \quad (11)$$

where  $n_i$  is the number density of colliding molecules (i), and  $\gamma_{oi}$  is the semi half width at reference conditions  $T_o$ ,  $n_o$ ,  $P_o$ , which are taken as standard temperature and density and pressure.  $\gamma_{oi}$  is a quantity which must

be determined experimentally, and which in general depends on the colliding partner(i), since the collisional line broadening depends on the forces between the radiating molecule and the colliding molecule. It is the purpose of the present experimental work to determine  $\gamma_{oi}$  for  $i = N_2$  and  $i = \text{air}$ , for each of the lines  $\lambda 5106$  and  $\lambda 5153$  of Cu.

Although a complete expression for  $\gamma_{oi}$  cannot be derived without a knowledge of the intermolecular potential involved, Lorentz obtained a relation in terms of a hard-sphere model of interaction with an "optical collision diameter",  $\rho_i$ . The full line width at half height,  $2\gamma_{oi}^v = \frac{c}{\lambda^2} (2\gamma_{oi}^h)$  may be written in terms of the mean free path,  $L$ , and the average particle velocity,  $v$ , as

$$2\gamma_{oi}^v = \frac{v}{\pi L} = \frac{P}{kT} \sqrt{\frac{8kT}{\pi m}} \rho_i^2$$

After substitution and rearranging,  $\gamma_{oi}^h$  may be written as

$$\gamma_{oi}^h = \sqrt{\frac{2}{\pi}} \lambda^2 \frac{n_o}{c} \left( \frac{RT_o}{M_i} \right)^{1/2} \rho_i^2$$

where  $\lambda$ ,  $\gamma$  and  $\rho_i$  are measured in cm,  $c = 3 \times 10^{10}$  cm/sec,  $R = 8.314 \times 10^7$  ergs/°K mole and  $M_i$  is the molecular weight of the reduced mass of the radiating and colliding molecules. For Cu -  $N_2$  collisions (and approximately, Cu Air),  $M_i = 19.4$  gms/mole, and for  $\lambda = 5.1 \times 10^{-5}$  cm this becomes

$$\gamma_{oi}^h (\text{cm}) = 6.35 \times 10^4 (\rho_i (\text{cm}))^2 \quad (12)$$

Previously reported<sup>8</sup> values for  $\rho_i$  for Cu in  $N_2$  are of order  $5\text{\AA}$ , so that the pressure broadened lines could be expected to have a value of  $\gamma_{oi}$  of about  $\gamma_o \sim 0.02\text{\AA}$ . For test conditions of 70 atm pressure and a temperature of  $6000^\circ\text{K}$ , this would result in a line half width of  $\gamma_c \sim 0.3\text{\AA}$ , which is the order of the observed widths.

8. Ovechkin, G.V. and Sandrigailo, L.E. Line Broadening and Shift in an Arc for Low Copper Contents, J. Applied Spectroscopy (USSR), 10, 565, April 1969.

Inspection of the anticipated line widths from each of these sources shows clearly that the measured broadening can be related solely to collisional effects. Accordingly the data were reduced with this interpretation, and were utilized to determine  $\gamma_{oi}$ .

#### 5.1.5 Line Shift

As a result of collisions, the copper lines are not only broadened but are also shifted in wavelength. Lindholm<sup>(9)</sup> has analysed the magnitude of the broadening and the shift to be expected from a collisional interaction potential of the form

$$\Delta V = - \frac{h}{2\pi} \frac{C_n}{R^n}$$

where  $C_n$  is the interaction constant,  $R$  is the distance to the perturbing particle and  $n$  characterizes the type of interaction. Perturbation by neutral particles is due to van der Waal forces and corresponds to  $n = 6$ . For a van der Waal type of potential, Lindholm<sup>(9)</sup> obtained

$$2\gamma = \frac{8.16}{2\pi} \frac{\lambda^2}{c} C_6^{2/5} v^{3/5} n_i, \quad \Delta_6 = \frac{2.96}{2\pi} \frac{\lambda^2}{c} C_6^{2/5} v^{3/5} n_i$$

where  $2\gamma$  is the full half-width of the spectral line, and  $\Delta_6$  is the shift of the line center.  $v$  is the collisional velocity,  $n_i$  the number density of colliding molecules and  $c$  is the speed of light. The dimensions of  $C_6$  are then  $\text{cm}^6/\text{sec}$ .

An equation relating  $C_6$  to the measured line width and gas temperature and number density can be obtained by using the relation for the average velocity

$$v = \left( \frac{8RT}{\pi M} \right)^{1/2}$$

so that

$$\gamma = \frac{8.16}{4\pi} \frac{\lambda^2}{c} C_6^{2/5} \left( \frac{8RT}{\pi M} \right)^{3/10} n_i$$

9. Lindholm, E., Arkiv Mat., Astr., Fys., 28B, No. 3 (1941).

Thus the Lindholm theory predicts a temperature dependence for  $\gamma$  of  $T^{0.3}$  rather than  $T^{0.5}$ , as given by Lorentz (equation 11). Of special interest in the Lindholm theory is the fact that a fixed value is predicted for the ratio of the full line half width to line shift. For the  $R^6$  potential this is

$$\frac{2\gamma}{\Delta_6} = \frac{8.16}{2.96} = 2.8 \quad (13)$$

### 5.1.6 Thick-Gas Effects for Collision-Broadened Lines; Intensity Ratios

For a collision-broadened line the shape of the absorption coefficient curve is known, viz

$$k(\lambda) = \frac{S \gamma_c}{\pi} \frac{1}{(\lambda - \lambda_0)^2 + \gamma_c^2} \quad (14)$$

so that equation (3) can be integrated to obtain  $W$  as a function of  $Su$  and  $\gamma_c$ , and tabulated results are available. Various analytic relations have been suggested to fit the tabulated results with various degrees of accuracy and complexity.<sup>10</sup> A relatively simple relation that is accurate within 10% is

$$W = \frac{Su}{\sqrt{1 + \frac{0.25 Su}{\gamma_c}}} = \frac{Su}{\sqrt{1 + X}} \quad (15)$$

The parameter  $X \equiv \frac{0.25 Su}{\gamma_c}$  describes the optical thickness, and the gas is optically thin if  $X \ll 1$ . Equation (15) can then be used in equation (2) to describe the line radiance of a collision-broadened optically thick line. Using equations (2) and (15) an expression can be obtained for the ratio of the radiance of two spectral lines A and B:

$$\frac{N_A}{N_B} = \frac{N_A^0}{N_B^0} \frac{(Su)_A}{(Su)_B} \sqrt{\frac{1 + \left(\frac{0.25 Su}{\gamma_c}\right)_B}{1 + \left(\frac{0.25 Su}{\gamma_c}\right)_A}} = \frac{N_A^0}{N_B^0} \frac{(Su)_A}{(Su)_B} \sqrt{\frac{1 + X_B}{1 + X_A}} \quad (16)$$

Comparing this expression with equation (8) for a thin gas, we see

$$\frac{N_A}{N_B} = \left(\frac{N_A}{N_B}\right)_{\text{THIN}} \sqrt{\frac{1 + \left(\frac{0.25 Su}{\gamma_c}\right)_B}{1 + \left(\frac{0.25 Su}{\gamma_c}\right)_A}} = \left(\frac{N_A}{N_B}\right)_{\text{THIN}} \sqrt{\frac{1 + X_B}{1 + X_A}} \quad (17)$$

10. Ludwig, C.B., Malkmus, W., Reardon, J.E. and Thomson, J.A. Handbook of Infrared Radiation From Combustion Gases. NASA SP-3080, (1973).

Thus a line which is strong ( $S_u$  large) and narrow ( $\gamma_c$  small) compared with a second line will be weakened (relative to the second line) by thick-gas effects.

From equations (5) and (11) it is seen that the optical thickness parameter can be evaluated, for  $\ell$ ,  $\lambda$  and  $\gamma$  in cm, as

$$\chi \equiv \frac{0.25 S_u}{\gamma_c} = \frac{0.25 \times 3.57 g_u A \lambda^4 \ell}{\gamma_o} \cdot 10^7 \frac{\left(\frac{n_{cu}}{n_o}\right) e^{-E_l/kT}}{\left(\frac{n_o}{n_o}\right) \sqrt{\frac{T}{T_o}}} \quad (18)$$

#### 5.1.7 Effects of Finite Slit Width on Measured Line Width

The radiation received at a given wavelength setting of the spectrometer depends not only on the radiation emitted by the gas at that wavelength, namely

$$N_\lambda = N_\lambda^o \left(1 - e^{-k(\lambda)u}\right)$$

but also on the slit function of the spectrometer,  $\sigma(\lambda, \lambda')$ , which represents the fraction of radiation of wavelength  $\lambda'$  that is transmitted by the spectrometer when the latter is set at wavelength  $\lambda$ . Then the radiation observed at wavelength  $\lambda$  is

$$N_{\lambda_{obs}} = \frac{N_\lambda^o \int \sigma(\lambda, \lambda') \left(1 - e^{-k(\lambda')u}\right) d\lambda'}{\int \sigma(\lambda, \lambda') d\lambda'}$$

or

$$N_{\lambda_{obs}} = N_\lambda^o \left\{ 1 - \frac{\int \sigma(\lambda, \lambda') e^{-k(\lambda')u} d\lambda'}{\int \sigma(\lambda, \lambda') d\lambda'} \right\}$$

These integrals have been evaluated numerically in Reference (11) for pressure-broadened line shapes  $k(\lambda)$  (Eqn. (14)), and Gauss-function slit shapes  $\sigma(\lambda, \lambda')$ . If  $\delta\lambda$  is taken as the half-width at half-height of the slit function, the relation between the observed line half width ( $\gamma_{OBS}$ ) and the true line half width ( $\gamma$ ) has been determined as a function of  $\delta\lambda$  for the case of  $e^{-k(\lambda_0)u} = 0.7$ , or  $k(\lambda_0)u = 0.36$ . This would correspond to a line that is close to optically thin ( $0.7 \simeq 1-0.36$ ). The results are shown in Figure 5, adapted from Figure 1 of Reference 11, and will be used in the discussion of measured line widths in Section 5.3.

## 5.2 RELATIVE TRANSITION PROBABILITY OF THE 5106Å AND 5153Å COPPER LINES

Representative tracing of oscilloscope records of the output of the opacity monitor during the relative transition probability measurements are shown in Figure 6. The output signals from the two channels viewing the 5106Å copper line are seen to be essentially the same. Furthermore, the signal levels for the reflecting wall (Fig. 6(b)) and non reflecting wall (Fig. 6(a)) are seen to be in the ratio of about 2 to 1. This ratio is consistent with the performance of the relative transition probability measurements under optically thin conditions (Section 3.1). The relative transition probability measurements were performed using 0.005 in. diameter copper wire. Initial wire lengths of about 20 mm were investigated, the wire lengths then being progressively reduced to the order 2-5 mm in subsequent tests until the opacity-monitor signal levels attained the desired ratio indicative of optical thinness.

Typical data records of the output of the transition probability radiometers are illustrated in Figure 7. It is noted that, except for the first 100  $\mu$ sec of the 5153Å radiation channel, the copper line intensity levels are essentially constant. These data, together with measured corrections for background radiation levels, therefore enabled consistent and unambiguous relative line-intensity values to be obtained.

11. Kostkowski, H.J. and Bass, A.M. Slit Function Effects in the Direct Measurement of Absorption Line Half-Widths and Intensities. J. Opt. Soc. Am., 46, 1060, December 1956.

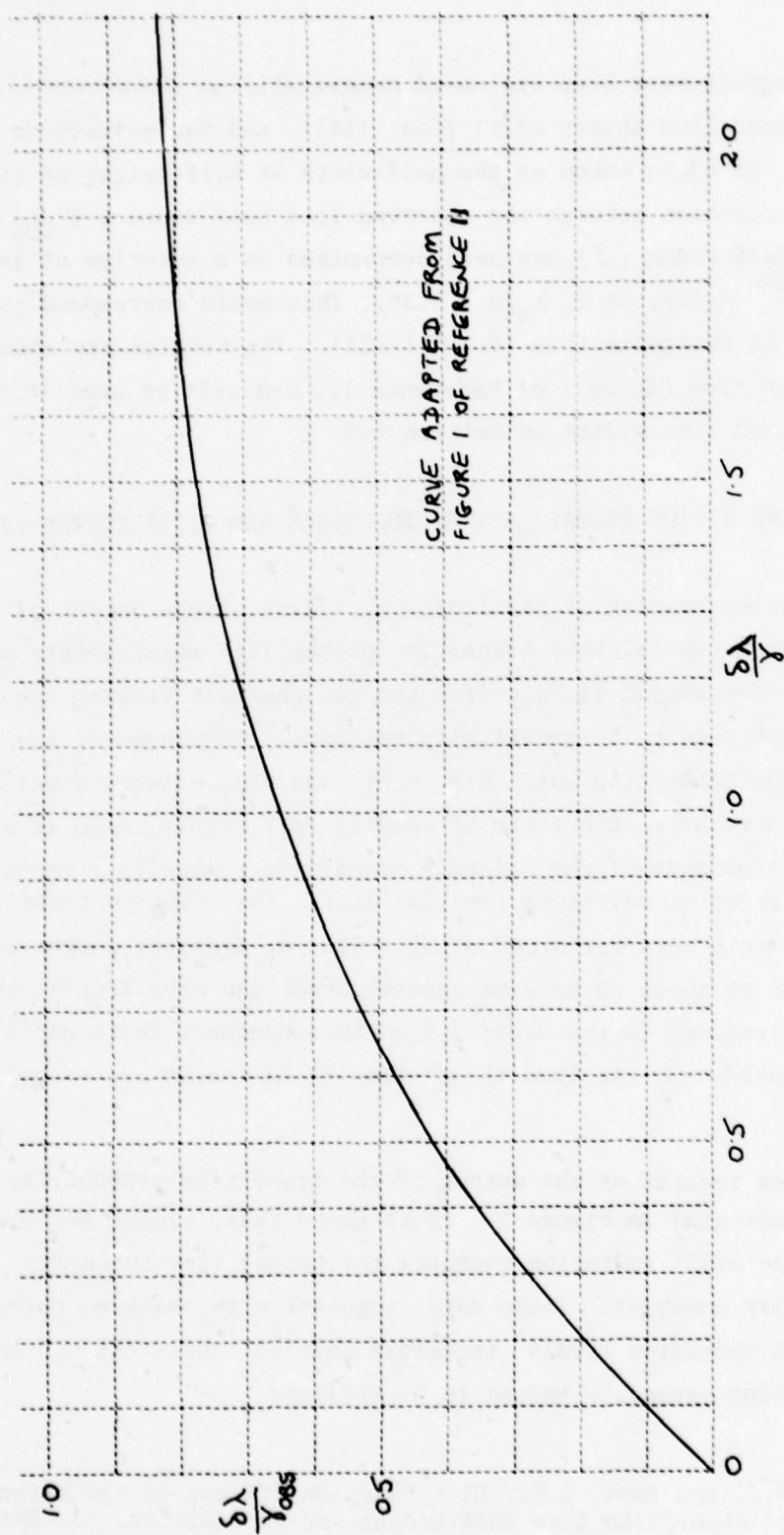
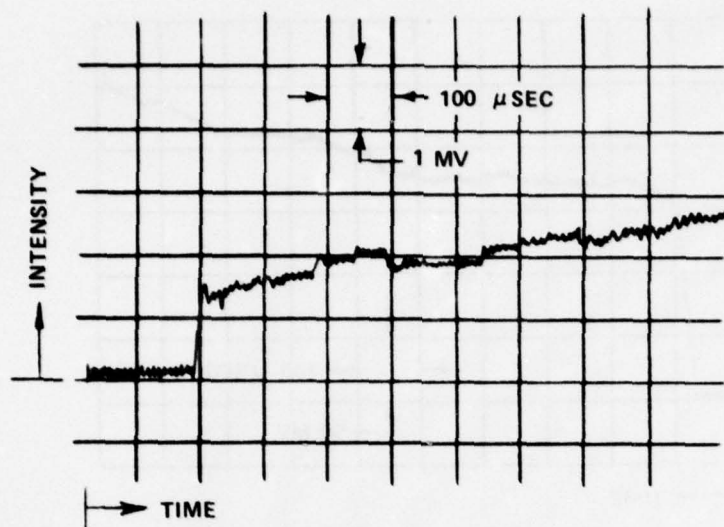
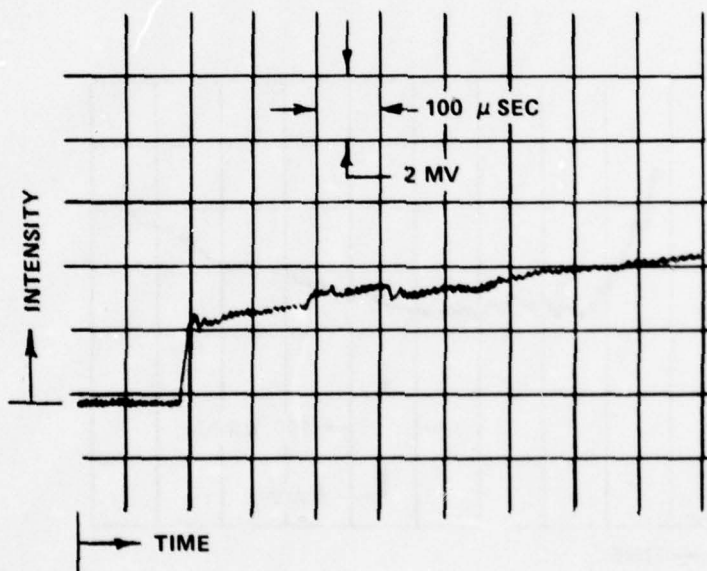


Figure 5. RATIO OF SLIT FUNCTION HALF WIDTH AT HALF HEIGHT TO LINE HALF WIDTH AT HALF HEIGHT - OBSERVED VS. TRUE (COLLISION-BROADENED LINE, GAUSSIAN SLIT FUNCTION)

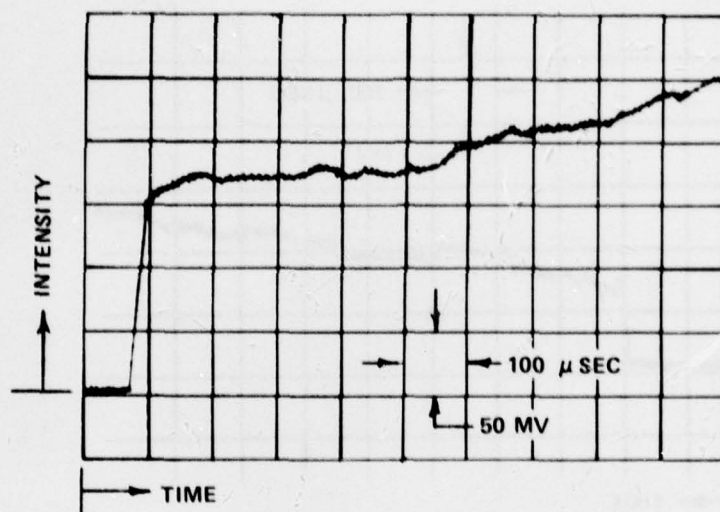


(a) NON REFLECTING WALL

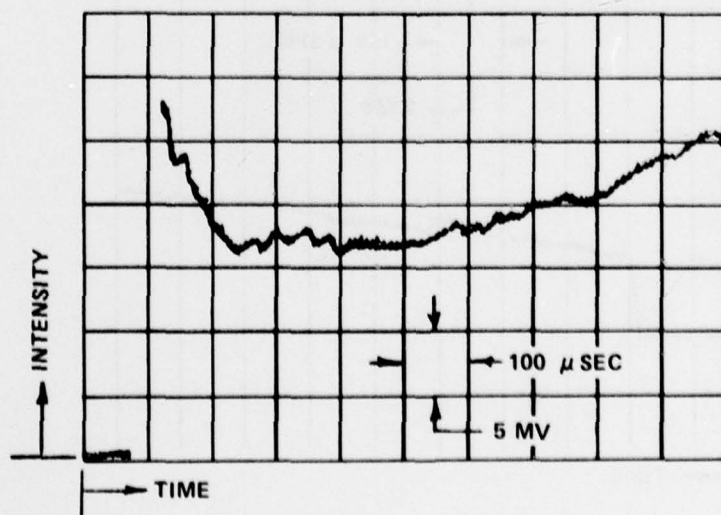


(b) REFLECTING WALL

Figure 6. TYPICAL TRACES FROM THE OPACITY MONITOR VIEWING THE  $5106\text{\AA}$  ATOMIC COPPER LINE



(a) 5106 Å ATOMIC COPPER LINE



(b) 5153 Å ATOMIC COPPER LINE

Figure 7. OUTPUT OF TRANSITION PROBABILITY RADIOMETERS.  
EQUILIBRIUM GAS TEMPERATURE = 4030°K

The difference in the initial (100  $\mu$ sec) response evident in the records of Figure 7 was examined further in a dedicated series of runs. The initial behavior was examined by arranging for both radiometer optical systems to view the 5106A line simultaneously, and subsequently the 5153A line, in several repeat experiments. In all cases, the radiation intensity records, in each run, were essentially identical. This corroborated the separate optical-bench calibration of the instrument in that the time response and sensitivity of each radiometer channel was the same. However, the difference in the initial response of each radiometer channel remained as illustrated in Figure 7.

Further explanation of this phenomenon was not pursued because this initial behavior did not compromise the useful data. It is also noted that similar behavior was also observed in the radiometer instrument records obtained during the line-width measurements to be discussed (e.g. Figure 14).

A slight increase in line-radiation intensity is evident in the radiometer records of Figure 7. This increase may be associated with a variation in concentration of copper atoms or a temperature variation, or both. If this variation is interpreted in terms of atomic copper concentration, the optically thin requirement for these tests is not violated and the relative intensity ratio remains constant. On the other hand, if it is assumed that all of the variation is due to temperature change, the temperature variation can be estimated, since the radiation intensity near 5000A varies approximately with the 7th power of the temperature. Such estimates have been made and the uncertainty in temperature lies well within the temperature uncertainty indicated below for the final results. Actually, it appears that both effects may exist as evidenced by the near parallelism of the oscilloscope traces.

The results of all of the measurements for the relative intensity of the 5106 and 5153Å copper lines were corrected for background radiation and normalized to a temperature of 4000°K. The actual shocked-gas temperatures ranged from 4000 to 4070°K. The data are shown in Figure 8, together with values taken from the literature.<sup>7</sup> The vertical bar indicates the scatter in the normalized radiation-ratio data. The horizontal bar indicates the uncertainty in the calculated shock-gas temperature due to wave speed round-off, extrapolated wave speed attenuation, and computational input data. As can be seen, the present data lie between the values of Kock and Richter,<sup>12</sup> and Corliss and Bozman.<sup>13</sup> The thin-line temperature dependence of the relative intensities of these two lines, as given by equation (8), is shown by the dashed curve, with the constant  $\frac{(g_u A)_{5153}}{(g_u A)_{5106}}$  fitted to the experimental determination at 4000 K. This ratio is

$$\frac{(g_u A)_{5153}}{(g_u A)_{5106}} = 4.1 \pm 4$$

The dashed curve thus represents the suggested curve to be used in deducing gas temperatures from the measured ratio of intensities of these two lines, based on the present measurements. For comparison, the values of  $g_u A$  given for these transitions in Section 5.1.1, Table 1 yield a ratio

$$\frac{(g_u A)_{5153}}{(g_u A)_{5106}} = 3.1$$

The data shown near 5900°K were taken during the line-width measurements and are discussed in Section 5.3. They fall very close to the dashed curve, but may be influenced by thick-gas effects as discussed in Section 5.3.1.

12. Kock, M. and Richter, J., Experimental Transition Probabilities and the Solar Abundance of Copper, *Zeitschrift Fur Astrophysik*, 69, 180, (1968).
13. Corliss, C.H. and Bozman, W.R., Experimental Transition Probabilities for Spectral Lines of Seventy Elements, NBS Monograph 53, (1962).

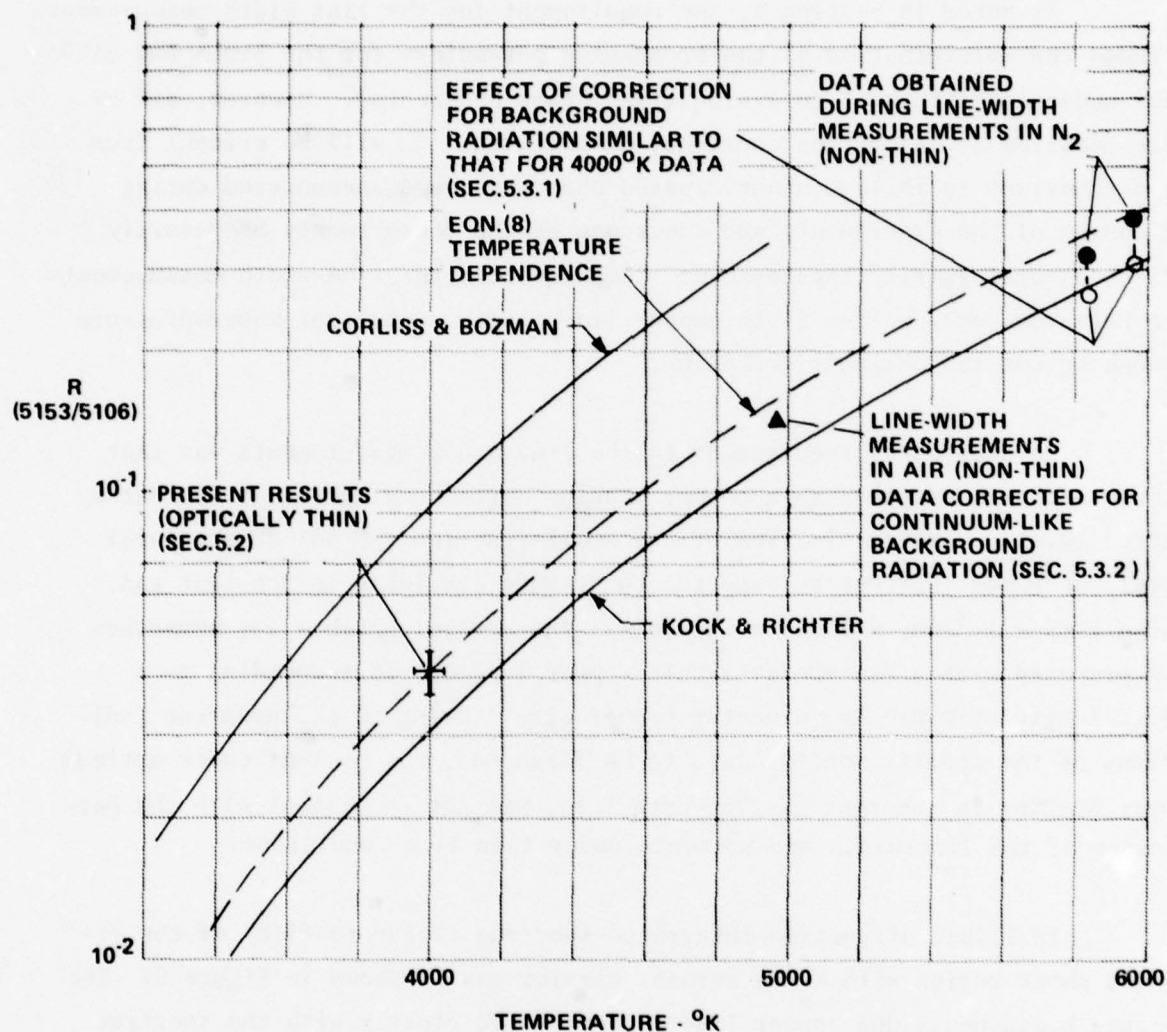


Figure 8. RATIO,  $R$ , OF INTENSITY OF 5153Å TO 5106Å LINES OF ATOMIC COPPER

As noted in Section 1, the requirement for the line width measurements included the determination of the broadening parameters for the 5106A and 5153A lines under conditions of collisional and Stark broadening. However, all of these measurement objectives could not be achieved. As will be evident from the discussions to follow, unanticipated phenomena were encountered during the course of the experiments and the scope of the measurements necessarily reflected some priority reassessment. Consequently the line-width measurements were performed only on the 5106A copper line, under conditions where pressure broadening was the dominant mechanism.

An additional requirement in the line-width measurements was that primary emphasis be given to a copper loading corresponding to a 0.1% contamination level. However, in view of the small fraction ( $\leq 5\%$ ) of the total copper vaporized that can be expected to be made available in the test gas, such a copper loading was not attainable. The aerosol chamber was nevertheless prepared with a maximum available copper loading, corresponding to a 0.9 in. length of 0.010 in. diameter copper wire. Owing to the apparent indications of the opacity monitor data to be discussed, the present under-optimum copper loading in the test gas, nevertheless, was not consistent with the performance of the line-width measurements under thin line conditions.

An illustrative time-integrated spectrum (Polaroid film) of the reflected shock region with  $N_2$  as aerosol carrier gas is shown in Figure 9. The pressure broadened 5106A copper line is contrasted clearly with the spectrum from the hollow-cathode copper source. The less-intense 5153A line is also evident although its clarity in definition has been somewhat compromised in the photograph reproduction.

As noted, the line-width measurements were performed using both  $N_2$  and air as the Cu-aerosol carrier gases and at pressure levels, in each case, which differed by about a factor of two. In order to ensure valid comparisons of the line-profile scan data obtained in separate experiments, it was

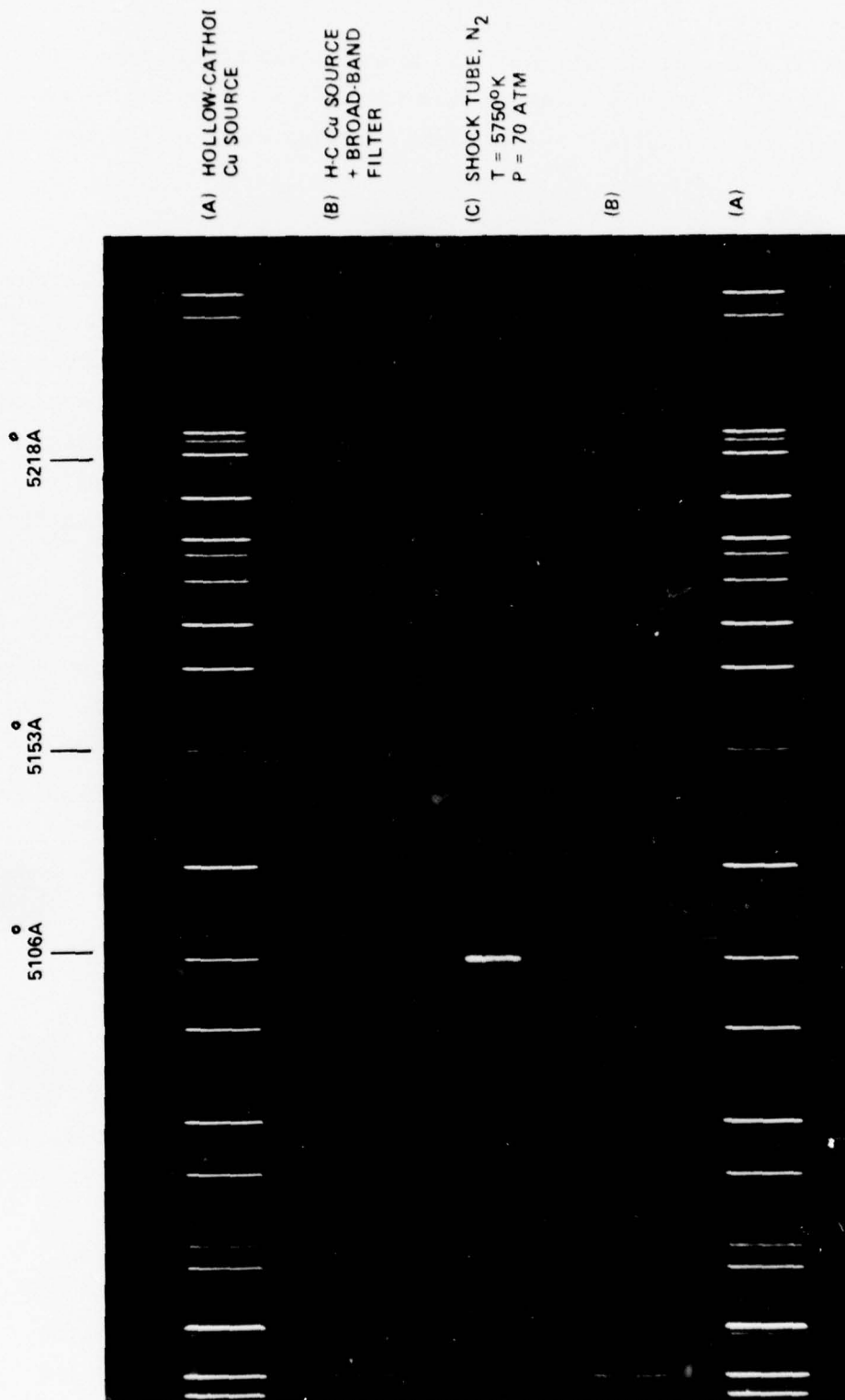


Figure 9. COMPARISON OF TIME-INTEGRATED SPECTRA FROM SHOCK TUBE AND HOLLOW-CATHODE COPPER SOURCE. N<sub>2</sub> CARRIER GAS

therefore essential that the operation of the scanning spectrometer be consistent and repeatable. Any variation in scan-mirror speed from run to run, for example, would directly affect the apparent measured width of the spectral line.

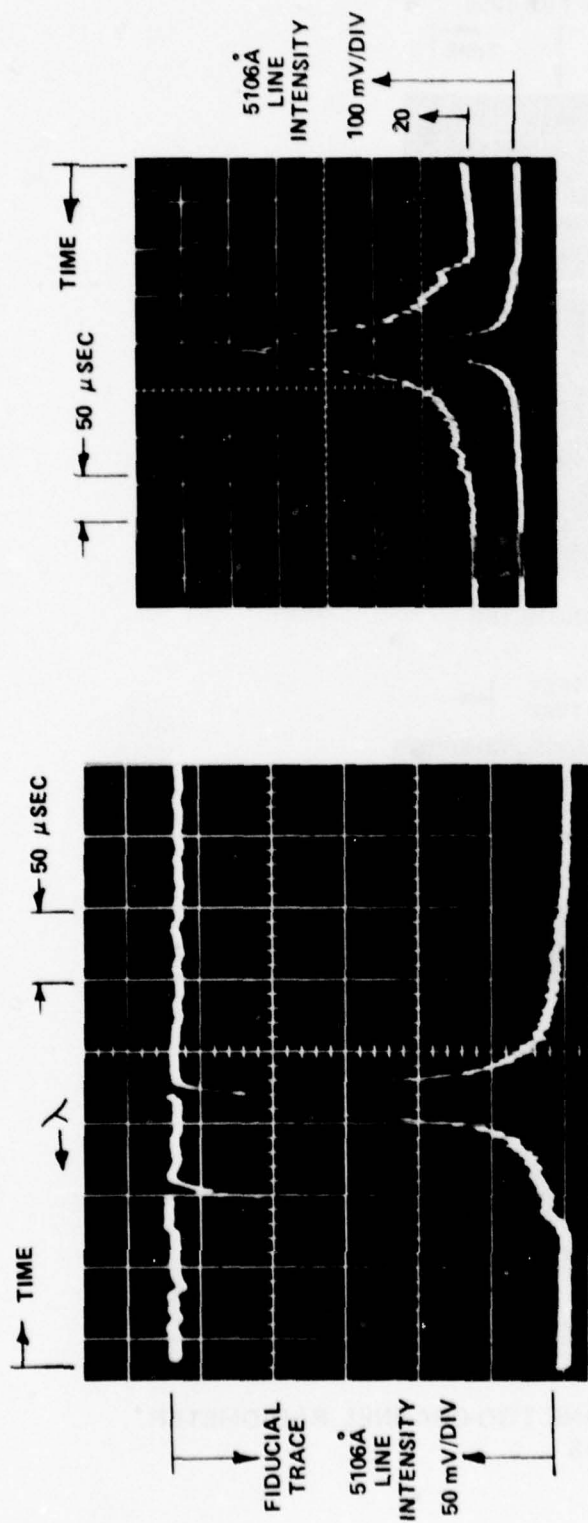
In order to monitor the operation of the scan mirror system, a He-Ne laser source was employed with the laser light reflected from a section of the scan mirror. The reflected laser beam was then directed to scan across a grid ruling located in front of a photomultiplier. The photomultiplier output, as a mirror-speed fiducial trace, was displayed on both the spectrometer scan and the radiometer records. The former enabled verification of constancy of scan speed from run to run, and the latter permitted temporal identification of the line scan within the test-time interval. Excellent repeatability of scanner operation was corroborated in the experiments.

On the basis of the instrument function measurements performed using the Hg 5461Å line, and the measured slit sizes of the spectrometer (Section 4.2), the present Cu line-scan measurements, referred to the oscilloscope records (e.g. Figures 10, 13) were recorded at  $3.4 \times 10^{-2} \text{ Å}/\mu\text{sec}$ . Prior to each test, a scan of the Hg green (5461Å) line was routinely recorded as a check on mirror scan speed and the measured half width at half-height of the Hg line.

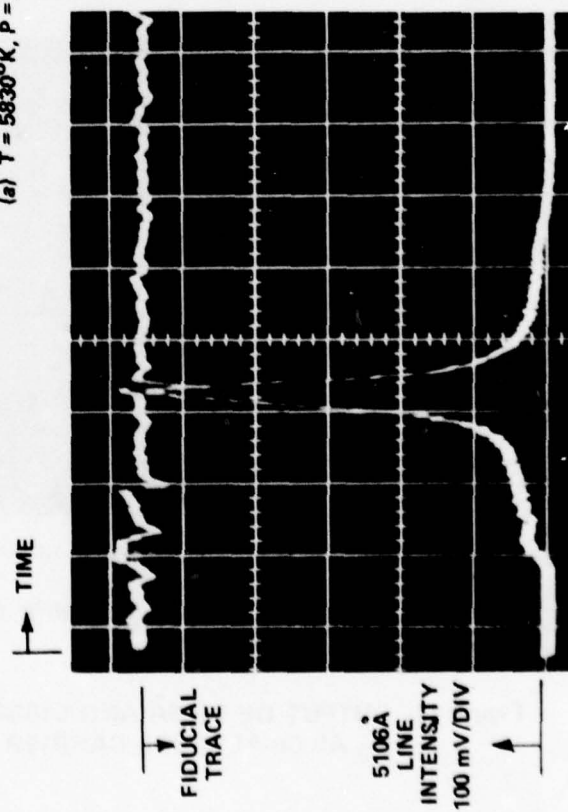
#### 5.3.1 N<sub>2</sub> As Carrier Gas

Spectral scans of the 5106Å copper line are shown in Figure 10. These data were obtained at reflected shock pressures of 35.7 and 70.0 atm., at a reflected shock temperature of about 5900°K.

The output of the two-channel radiometer monitoring the 5106Å and 5153Å copper line radiations is shown in Figure 11 for the 35.7 atm. run condition. The test period immediately following the arrival of the reflected shock in Figure 11 is seen to be sensibly uniform for a period of about 150 μsecs. In addition, reference to the corresponding fiducial traces in

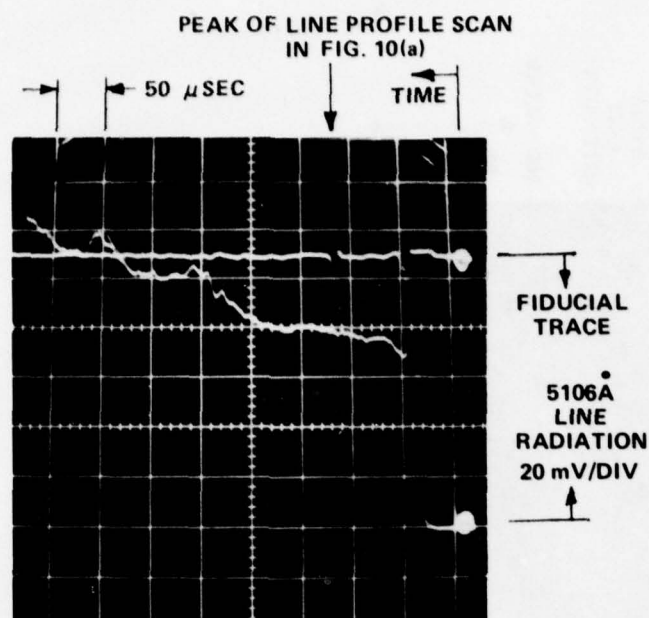


(a)  $T = 5830^{\circ}\text{K}$ ,  $P = 35.7 \text{ ATM}$

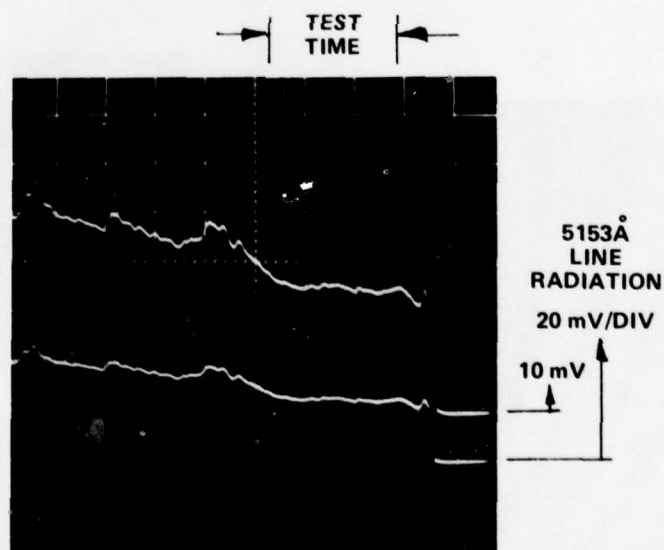


(b)  $T = 5960^{\circ}\text{K}$ ,  $P = 70.0 \text{ ATM}$

Figure 10. SPECTRAL SCANS OF THE 5106 Å COPPER  
ATOMIC LINE.  $\text{N}_2$  AS CARRIER GAS



(a) 5106 Å LINE RADIOMETER



(b) 5153 Å LINE RADIOMETER

$T = 5830^{\circ}\text{K}$ ,  $P = 35.7 \text{ ATM}$

Figure 11. OUTPUT OF 5106 Å AND 5153 Å LINE TWO-CHANNEL RADIOMETER.  
 $\text{N}_2$  AS Cu-AEROSOL CARRIER GAS

Figures 10(a) and 11(a) shows that the line profile scans were performed, as desired, in the middle of the uniform test-time interval. The ratio of these measured intensities is plotted in Figure 8, and is discussed later in this section.

The measured half-height line half widths  $\gamma_{\text{OBS}}$ , corresponding to the 5106Å line scan records of Figure 10 are  $0.27 \pm 0.04\text{Å}$  and  $0.37 \pm 0.04\text{Å}$  for the 35.7 and 70 atmosphere pressure conditions respectively. To correct these measured values for the effect of finite slit width reference is made to the slit width measurements described in Section 4.2. The effective half width at half height of the slit function of the spectrometer was measured to be

$$\delta\lambda = 0.17 \text{ Å}$$

From the discussion of Section 5.1.7 and the graph of Figure 5 the measured values of the half widths at half height can then be corrected as given in Table 2.

TABLE 2  
Slit Width Correction for Measured  $\lambda_{5106}$  Line Half Widths

$T(^{\circ}\text{K})$	$P(\text{atm})$	$\gamma_{\text{OBS}}(\text{\AA})$	$\gamma_{\text{corrected}}(\text{\AA})$	$\frac{P/P_0}{\sqrt{T/T_0}}$	$\gamma_{0_1}(\text{\AA})$
5830	35.7	$0.27 \pm .04$	$0.18 \pm .06$	7.73	0.023
5960	70.0	$0.37 \pm .04$	$0.30 \pm .06$	15.0	0.020

The second last column gives the value of the parameter which scales the half-width and the last column gives the STP reference half width at half height (see equation 11). Using a value of  $\gamma_{0_1} = 0.021\text{\AA}$ , this results in an optical collision diameter (equation 12) of

$$\rho = 5.7\text{\AA}$$

The values in Table 2 can be compared with the data of Reference 8. In that reference (Table 2) the value of  $\gamma_0 = 2\gamma = 0.020\text{\AA}$  is given for test conditions of  $6000^{\circ}\text{K}$  and 1 atmosphere of  $\text{N}_2$  pressure. (The value for  $2\gamma$  given in Table 1 of Reference 8 is believed to be a typographical error.) According to equation 11, the corresponding value for 1 atm pressure that would be inferred from the data given here at  $5960^{\circ}\text{K}$  and 70 atm is  $2 \times 1/70$  of  $0.30\text{\AA}$ , or

$$2\gamma = 0.0086\text{\AA}$$

which is about 2.5 times less than the value indicated in Reference 8. If both results are taken at face value, this would throw serious doubt on the ability to scale line width directly with pressure over this large pressure range. A comparison of the Reference 8 value of  $0.020\text{\AA}$  at 1 atm and the present value of  $0.60\text{\AA}$  at 70 atm would indicate a pressure scaling of  $P^{0.80}$ .

The output signals from the opacity monitor viewing the  $5106\text{\AA}$  copper line at the  $\text{N}_2$  run condition of 35.7 atm. pressure are shown in Figure 12. The channel gains are identical and the photodiode detector response to a double-transit of the shock tube diameter (reflecting wall)

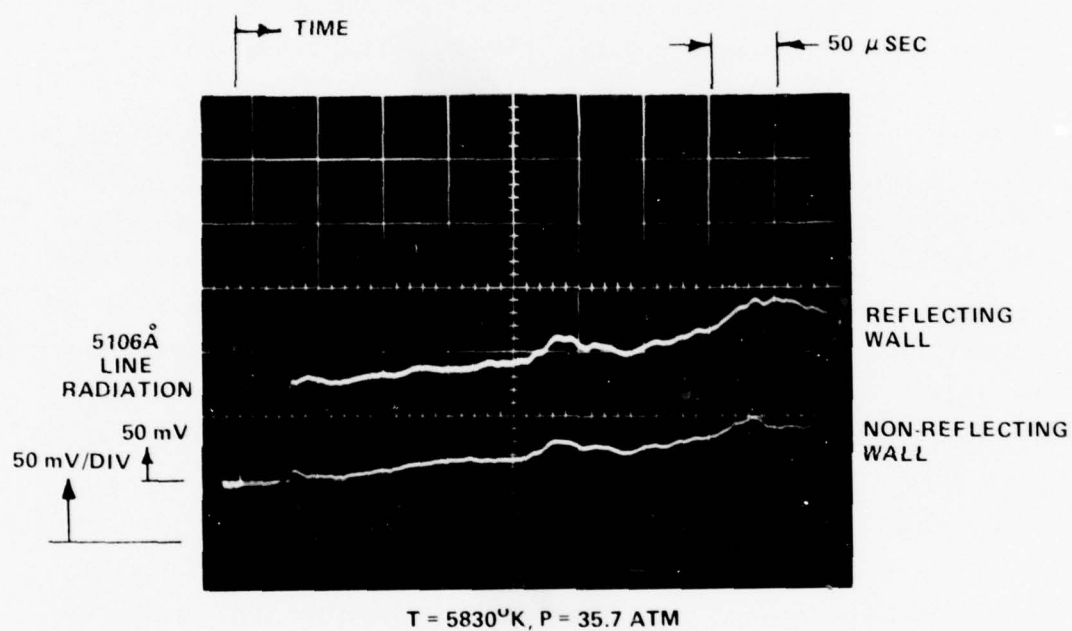


Figure 12. OUTPUT OF THE OPACITY MONITOR VIEWING THE 5106 Å Cu LINE.  
N<sub>2</sub> CARRIER GAS

is seen to exceed the signal for the photodiode viewing the non-reflecting wall. The ratio of the reflecting to non-reflecting wall signal levels in this case is 1.3, whereas for the optically thin condition, the ratio is calculated to be about 1.85 (e.g., Figure 6). The opacity monitor data for the higher pressure (70 atm.) condition were similar to those in Figure 12, with a signal level ratio of 1.5 at the slightly higher (by 130°K) temperature condition. Thus from these results it appears that the 5106Å copper line scans were performed under non-thin line radiation conditions.

The relative intensities of the 5106Å and 5153Å copper lines obtained from the two-channel radiometer measurements performed during the line-width experiments have also been included in Figure 8 for each of the test conditions in N<sub>2</sub>. As noted previously, no corrections for background radiation levels have been made in these data because of the commitment of the 3/4-meter spectrometer to the line-scan measurements. If a correction were made similar to that used for the 4000°K data, the ratio would be reduced about 20%, and this type of correction is indicated in Figure 8.

The data are nevertheless seen to locate closely to the curve through the thin-gas data obtained at 4000°K. The dashed curve is one prescribed by the calculated temperature dependence (Eqn. (8)) of the 5153/5106Å line relative intensity ratio under optically thin conditions, as noted in Section 5.2

To evaluate the effect of optical thickness on these two apparently contradictory results, it is necessary to know the line strengths, the line widths, and the copper concentration, as illustrated in equations (15), (17) and (18) of Section 5.1.6. Using the values for line strengths quoted in Section 5.1.1, the line width for  $\lambda_{5106}$  measured herein ( $\gamma_{o_i} = 0.024\text{Å}$ ) and a line width for  $\lambda_{5153} = \gamma_{o_i} = 0.05\text{Å}$  (Reference 8 gives a ratio of 2.5 for the two lines) the effect of optical thickness can be calculated as a function of copper number density.

Using equations (5) and (18), the following Table 3 can be generated for the two lines of interest, the nitrogen pressures and temperatures of the experiments and for pathlengths of one shock-tube diameter (7.62 cm) and two diameters (15.2 cm).

TABLE 3

Estimation of Effect of Optical Thickness

	$\lambda(\text{\AA})$	$T(^{\circ}\text{K})$	$p(\text{atm})$	$l(\text{cm})$	$Su/n_{\text{cu}} (\text{cm}^4)$	$X/n_{\text{cu}} (\text{cm}^3)$
a	5106	4000	32	7.62	$4.84 \times 10^{-24}$	$0.70 \times 10^{-15}$
b	5106	4000	32	15.2	$9.68 \times 10^{-24}$	$1.4 \times 10^{-15}$
c	5153	4000	32	7.62	$1.49 \times 10^{-25}$	$2.15 \times 10^{-17}$
d	5153	4000	32	15.2	$2.98 \times 10^{-25}$	$4.31 \times 10^{-17}$
e	5106	5830	35.7	7.62	$1.43 \times 10^{-23}$	$2.20 \times 10^{-15}$
f	5106	5830	35.7	15.2	$2.86 \times 10^{-23}$	$4.41 \times 10^{-15}$
g	5106	5960	70	7.62	$1.52 \times 10^{-23}$	$1.21 \times 10^{-15}$
h	5106	5960	70	15.2	$3.04 \times 10^{-23}$	$2.42 \times 10^{-15}$
i	5153	5830	35.7	7.62	$1.26 \times 10^{-25}$	$1.94 \times 10^{-17}$
j	5153	5830	35.7	15.2	$2.52 \times 10^{-25}$	$3.88 \times 10^{-17}$
k	5153	5960	70	7.62	$1.49 \times 10^{-25}$	$1.18 \times 10^{-17}$
l	5153	5960	70	15.2	$2.97 \times 10^{-25}$	$2.36 \times 10^{-17}$

The gas can be considered optically thin if  $X \ll 1$ , so that  $\sqrt{1+X} \sim 1$  in equation (15). Since  $n_{\text{cu}}$  is not known, it is not possible to obtain an accurate evaluation of  $X$ , but some idea can be obtained from the discussion of copper injection in Section 2.2. If the number density for the first set of experiments (4000 $^{\circ}$ K) is taken as  $10^{13} \text{ cm}^{-3}$ , it is clear that  $X \ll 1$  and these test conditions are optically thin, consistent with all the data. For the second set of experiments (5900 $^{\circ}$ K), if the number density of copper is taken as  $10^{15} \text{ cm}^{-3}$ , all the measurements of  $\lambda 5106$  would be optically thick ( $1.2 < X < 4.4$ ) and those of  $\lambda 5153$  would be thin ( $X < .04$ ). Thus the measurement of the ratio of the two lines would be affected by optical-thickness effects.

For example, the requirement that the opacity monitor measure  $\sim 1.6$  (after corrections for mirror losses) for  $\lambda 5106$  at 70 atm pressure (lines g and h of Table 3) can be used in equation (17) to evaluate X. Putting  $X_B = X$ , the value of X for line g of Table 3, and  $X_A = 2X$ , the value for line h, then

$$1.6 = 2 \sqrt{\frac{1+X}{1+2X}}$$

or  $X = 1.28$ , which corresponds to  $n_{cu} = 1.06 \times 10^{15} \text{ cm}^{-3}$ . Considering the ratio of intensities to be expected for  $\lambda 5153$  and  $\lambda 5106$ , this same value of  $n_{cu}$  can be used in lines g and k. For line g,  $X = X_B = 1.28$ . For line k,  $X = X_A = 0.013$ , and

$$\frac{N_A/N_B}{(N_A/N_B)_{\text{THIN}}} = \sqrt{\frac{1+1.28}{1+0.013}} = 1.5$$

Comparing this ratio with the departure of the high-temperature datum point in Figure 8 from the thin-gas curve, the discrepancy is considerably outside the limits of experimental error and is in the wrong direction from the thin-gas curve. Thus from these results we conclude that the opacity-monitor data and the line-ratio data are inconsistent at high temperatures, and that no firm conclusion can be drawn concerning the optical thickness or the copper number density for these experiments.

Also of interest is the effect of this self absorption on the measured line width. This can be examined numerically by using these same parameters in equation (14) to calculate the line shape  $ku$ , and then calculate the self-absorbed shape

$$(1 - e^{-ku})$$

for comparison of half-widths. The net effect is a 30% change in line width for line g. Thus it is concluded that if the self-absorption effects are as high as indicated by the opacity monitor, the half-widths given in Table 2 would be as much as 30% too large. From all of these considerations, it is felt that the most likely error is in the measurements that were made with the opacity monitor.

Finally, the question of observable line shift in the  $N_2$  data was investigated. A comparison of the positions of the 5106Å line between the hollow-cathode copper lamp and the shock tube source spectra in Figure 9, for example, shows no evidence of line shift. However, the definition of any fractional shift would be very difficult in this instance because of the lack of sharpness in the shock tube spectrum, due to overexposure, as well as the low dispersion. The photograph (Figure 9) is of a first-order spectrum, with a corresponding dispersion of about 9Å/mm.

Reference to the scan data of Figure 10, however, shows fairly clear evidence of a red shift of the 5106Å line center between the 35.7 atm and 70 atm data. This observation is made on the basis of the small, though evident, change in the register between the fiducial signature and the position corresponding to the line center in the scan profiles at the two pressure conditions.

As noted in Section 5.3, the fiducial signatures were simultaneously recorded on the scan profile data records. Their prime purpose was to monitor the constancy of scan mirror speed from run to run, i.e. constant fiducial spacing. Slight time jitter may occur in the location of the fiducials with respect to the graticule markings on the records from run to run, as a result of the reliance upon time delay units in transferring the scan-initiation signal from the shock tube heat transfer gauge signal. However, the relative positions of the line profile scan and the fiducial signal on the records is fixed, since both are effected by the scan mirror, unless a shift in the position of the line center occurs.

The measured shift to longer wavelength of the 5106Å line center from the 35.7 atm to the 70 atm test condition was  $0.13\text{Å} \pm 0.03\text{Å}$ . Thus the line shift that is inferred for 70 atmospheres is  $\Delta_6 = 0.26 \pm 0.06\text{Å}$ . In terms of the ratio of full width at half height ( $2\gamma$ ) to line-center shift ( $\Delta_6$ ) at the 70 atm test condition this corresponds to the value

$$\frac{2\gamma}{\Delta_6} = \frac{0.60 \pm .12}{0.26 \pm .06} = 2.3 \pm 0.9$$

which is close to the theoretical value of 2.8 for van der Waal forces given in equation (13) due to Lindholm<sup>(9)</sup>. It also agrees with the ratio measured by Ovechkin and Sandrigailo<sup>(8)</sup>.

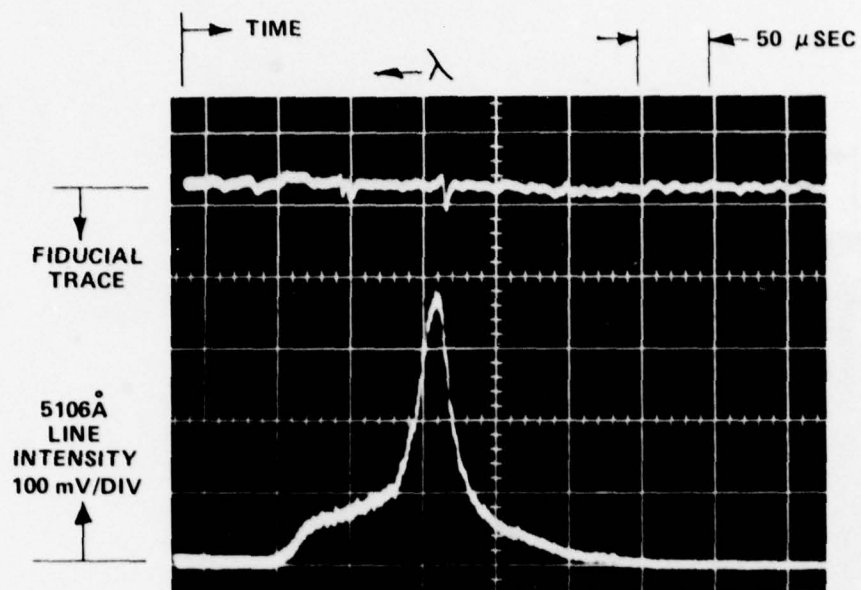
### 5.3.2 Air As Carrier Gas

Spectral scans of the 5106 $\text{\AA}$  copper line in air as the Cu-aerosol carrier gas are shown in Figure 13. The data represent the effect of a two-fold increase in reflected shock pressure, at a temperature of about 5000 $^{\circ}\text{K}$ .

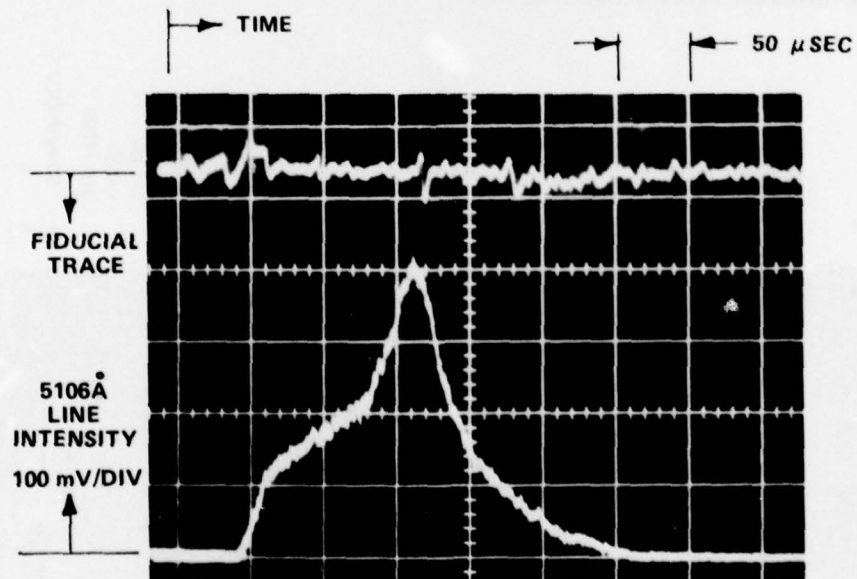
The two-channel radiometric data corresponding to the 90.3 atm. test condition are shown in Figure 14. The uniform test flow period, lasting about 150  $\mu\text{secs}$ , is clearly indicated, particularly in the channel monitoring the 5106 $\text{\AA}$  line radiation (Figure 14(a)). Note, however, that the initial response for the 5153 $\text{\AA}$  radiation is similar in the air case to that discussed previously for this wavelength channel in the relative transition probability measurements (Section 5.2), and shown in Figure 7. Temporal correspondence of the fiducial traces between Figures 13(b) and 14(a) also shows that the peak in the spectral scans was well located midway through the test-flow period.

The obvious feature in the line spectral scans of Figure 13, however, is the clear indication of an underlying continuum-like radiation upon which the Cu line radiation is superimposed. Apparent broadening of the copper line is clearly evident with increase in carrier gas pressure, although the measurements are obviously compromised by the presence of the background radiation.

Owing to its occurrence in the air spectral scan measurements, the background radiation would appear to be attributable to the presence of  $\text{O}_2$ . Accordingly, a repeat run at the 90.3 atm. test condition was made in air, without the addition of Cu-aerosol to the shock tube. The spectral scan record for this run is shown in Figure 15(a). Note that the signal gains differ by a factor of two between the scan records of Figures 13(b) and 15(a). The 5106 $\text{\AA}$  radiometer channel record for the pure-air case is also included, Figure 15(b), and is seen to be very similar to that for the corresponding case with Cu seeding shown in Figure 14(a), except for the level of the radiation signal.

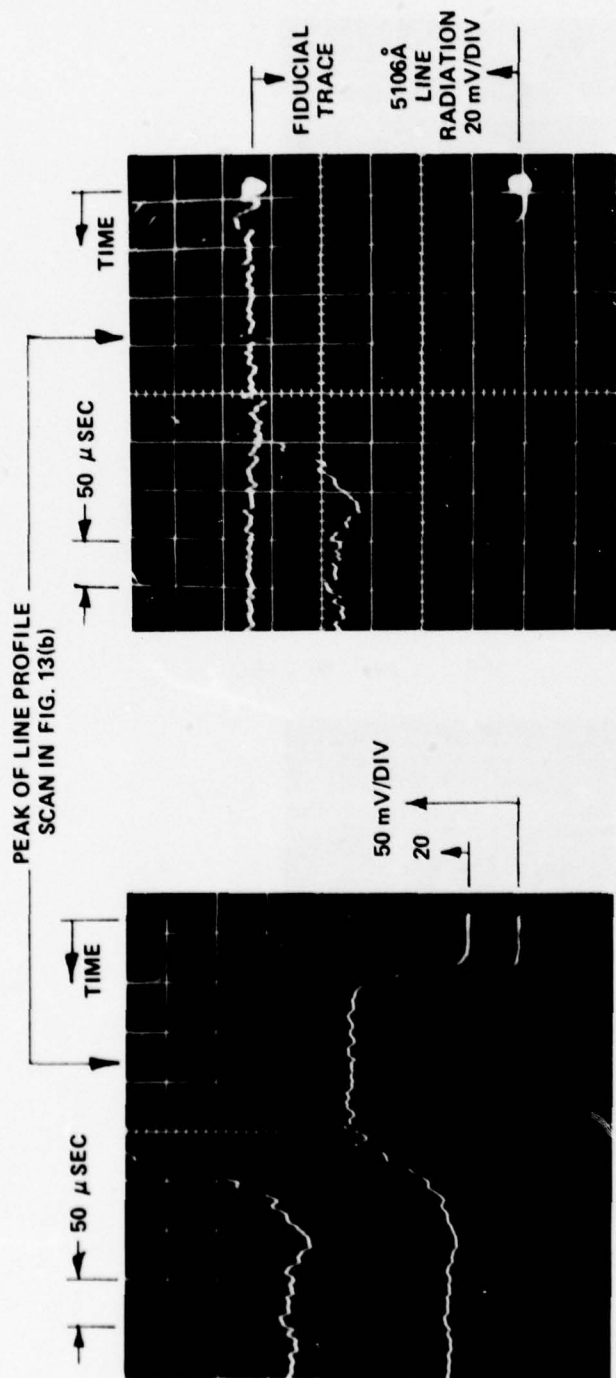


(a)  $T = 4975^{\circ}\text{K}$ ,  $P = 45.8 \text{ ATM}$

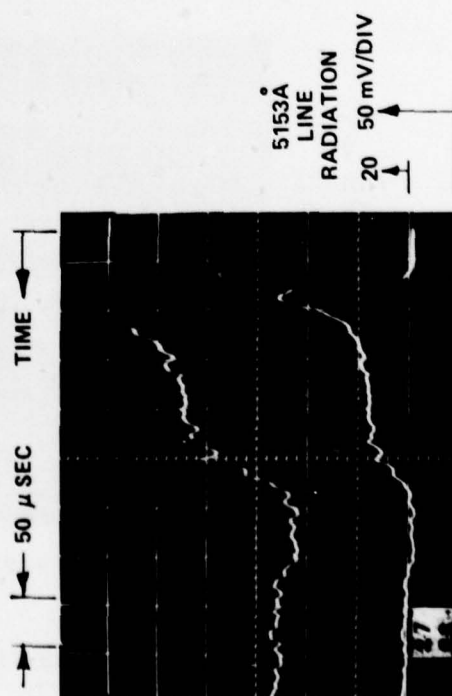


(b)  $T = 4970^{\circ}\text{K}$ ,  $P = 90.3 \text{ ATM}$

Figure 13. SPECTRAL SCANS OF THE 5106 Å COPPER ATOMIC LINE. AIR AS THE Cu-AEROSOL CARRIER GAS



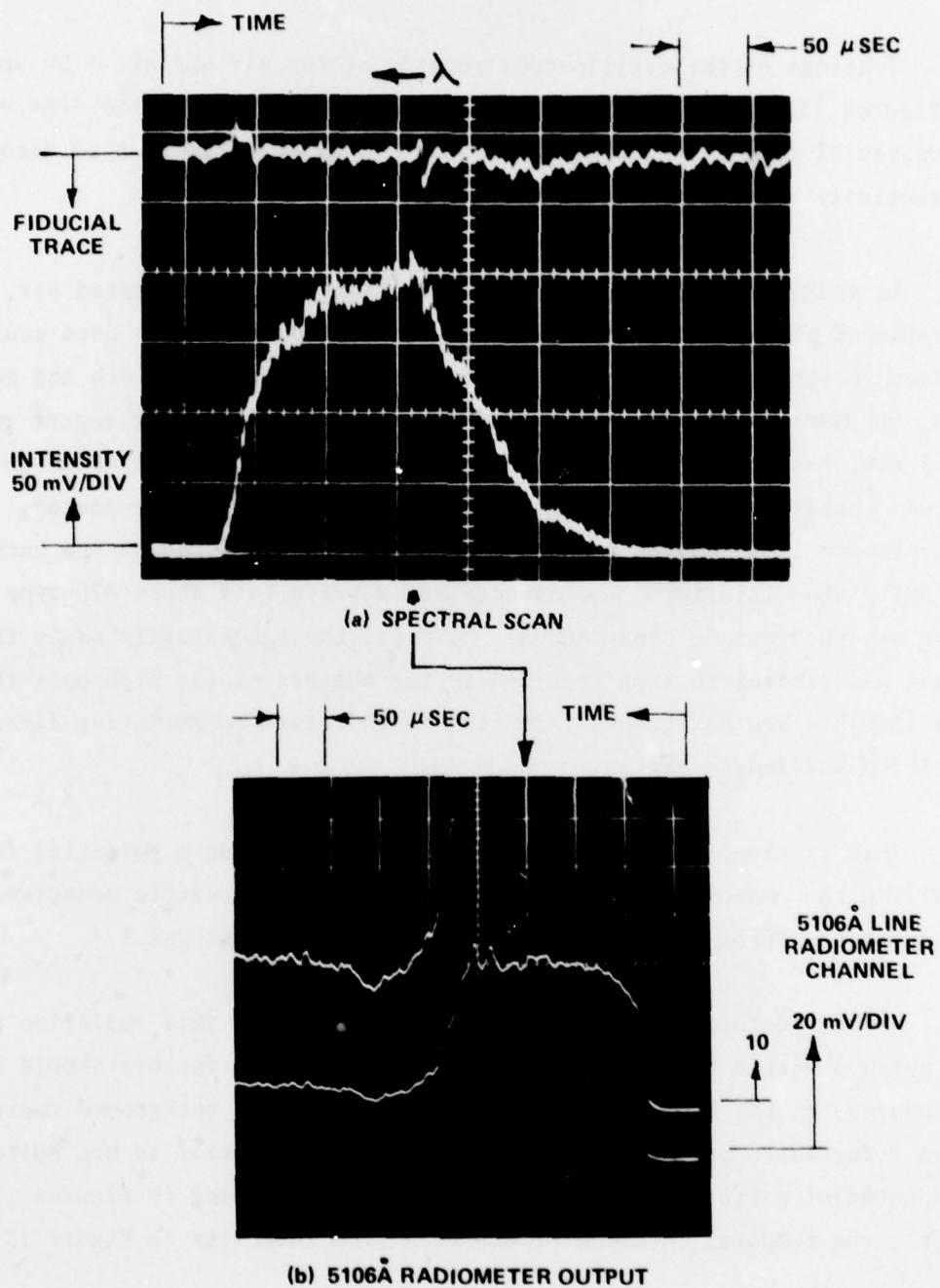
(a) 5106 $\text{\AA}$  LINE RADIOMETER



(b) 5153 $\text{\AA}$  LINE RADIOMETER

$T = 4970^{\circ}\text{K}$ ,  $P = 90.3 \text{ ATM}$

Figure 14. OUTPUT OF 5106 $\text{\AA}$  AND 5153 $\text{\AA}$  LINE TWO-CHANNEL  
RADIOMETER. AIR AS Cu-AEROSOL CARRIER GAS



$T = 4970^{\circ}\text{K}$ ,  $P = 90.3 \text{ ATM}$

**Figure 15. SPECTRAL SCAN AND RADIOMETER RESPONSE FROM REFLECTED SHOCK REGION IN PURE AIR**

Tracings of the oscilloscope records of the air and air + Cu scan data (Figures 13(b) and 15(a)) are reproduced in Figure 16 on the same scale for purposes of comparison. The background signal level is seen to account for essentially half of the total radiation signal in this case.

In seeking possible sources of radiation from shock-heated air, it was considered possible that contributions to the observed scan data could arise from shorter-wavelength radiation in higher order, e.g., 4th and 5th order  $O_2$  Schumann-Runge.<sup>14,15</sup> This was investigated in another repeat run at the 90.3 atm. test condition, in air + Cu aerosol, in which a 4500Å high-pass filter was installed at the entrance slit of the scanning spectrometer. The long-wavelength limit on instrument response was that imposed by the cathode of the EMI photomultiplier. The cathode was a tri-alkali whose S20-type response extended out to about 8000Å. However, the line-profile shape in this case was similar to that recorded in the absence of the high-pass filter (Figure 13(b)). The background radiation is therefore contributing directly in the 5000Å wavelength region.

This is clearly an important phenomenon and poses a potential for compromising the unambiguous use of the copper line radiometric measurement technique in the AFFDL RENT facility, with air as the test gas.

Further detailed investigation of the source of this radiation could not be pursued within the scope of the program. Several factors should be noted however, on the basis of the present results. The background radiation has been referred to as continuum-like, in that the behavior is not quite that expected of a true continuum. For example, referring to Figures 13(b) and 14(a), the temporal location of the peak line intensity in Figure 13(b)

14. Allen, R.A., Air Radiation Tables: Spectral Distribution Functions for Molecular Band Systems, AVCO Everett Research Report No. 236, April 1966.
15. Treanor, C.E. and Wurster, W.H., Measured Transition Probabilities for the Schumann-Runge System of Oxygen, J. Chem. Phys. 32, 758, 1960.

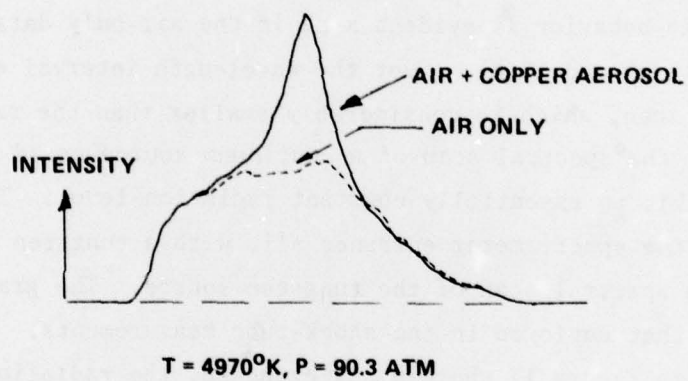


**Figure 16, SPECTRAL SCANS OF REFLECTED-SHOCK REGION IN AIR WITH AND WITHOUT COPPER AEROSOL**

is indicated on the corresponding radiometer record of Figure 14(a). The scan record (Figure 13(b)) exhibits a monotonic fall off in radiation intensity from the peak value. However, the radiation monitored within the 5106Å filter bandpass (Figure 14(a)) remains sensibly constant for a further 60-70  $\mu$ secs, i.e., during the period the scan signal data decreases by 75% from its peak value. Note that the direction of increasing time is opposite in the scan and radiometer records.

The same behavior is evident also in the air-only data, by comparison of Figures 15(a) and 15(b). Over the wavelength interval encompassed by the spectral scan, which is considerably smaller than the radiometer filter bandpass, the spectral scan of a continuum source could therefore be expected to exhibit an essentially constant radiation level. This was checked by illuminating the spectrometer entrance slit with a tungsten filament lamp and performing a spectral scan of the tungsten source. The grating setting was the same as that employed in the shock-tube measurements. The scan record is shown in Figure 17 wherein, as expected, the radiation is seen to be reasonably uniform over the wavelength interval of the scan. From these tests it thus appears that the background radiation cannot be attributed, at least unambiguously, to a continuum source.

Despite the peculiarities of the radiation behavior observed in the scan records as discussed above, the possible contribution of other air-continuum radiations, in the wavelength region pertinent to the copper line radiations, was nevertheless assessed. Two potential contributors would include the radiative recombination of  $\text{NO}_2$ , i.e.,



and the nitrogen first positive,  $\text{N}_2(1+)$ , band system. Both systems extend from the visible out to about 2  $\mu$ m.

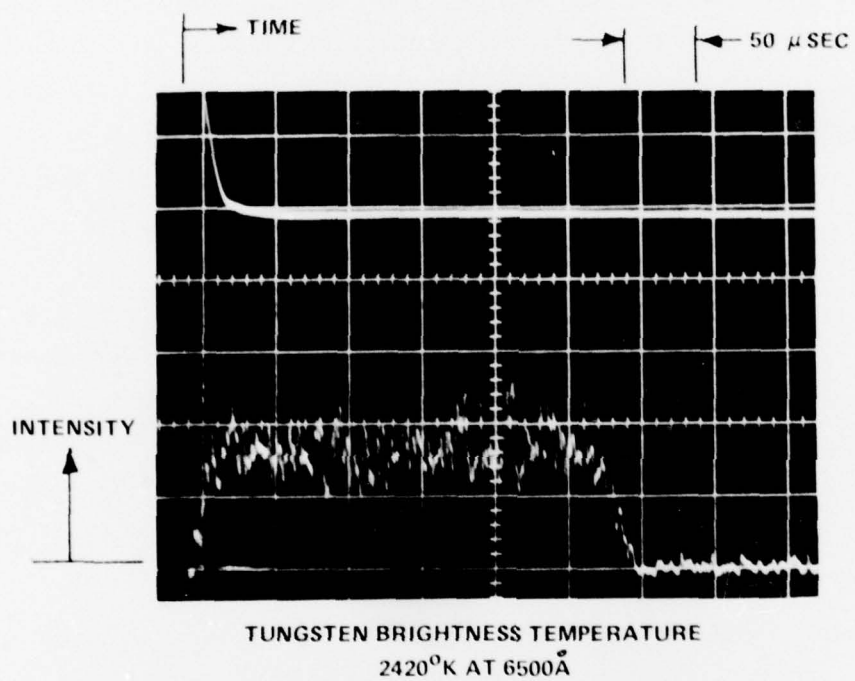


Figure 17. SPECTRAL SCAN OF TUNGSTEN SOURCE

In order to assess the possible contributions from these systems, the tungsten filament temperature was measured with an optical pyrometer. The brightness temperature, at  $6500\text{\AA}$ , was thus determined to be  $2420^\circ\text{K}$ , i.e., the tungsten filament was irradiating the spectrometer system, at  $6500\text{\AA}$ , like a blackbody at  $2420^\circ\text{K}$ . The ratio of the tungsten emissivities at  $5100\text{\AA}$  and  $6500\text{\AA}$  was obtained from DeVos,<sup>16</sup> as about 1.05, whence, at  $5100\text{\AA}$ , the tungsten source irradiated the system like a  $2800^\circ\text{K}$  blackbody. The scan data of Figure 17 then afforded an approximate calibration constant, from which a maximum radiance value of about  $680 \text{ w/cm}^2 \text{ sr } \mu\text{m}$  was estimated for the scan data in Figure 15(a).

The spectral radiance at  $5100\text{\AA}$ , from  $\text{NO}_2$  recombination in air at the reflected shock conditions corresponding to Figure 15 was evaluated from the data of Reference 17. It was found, however, that  $\text{NO}_2$  recombination accounted for only about 7% of the radiance estimated above for the pure-air scan data. Similarly, the  $\text{N}_2(1+)$  radiance at the same reflected shock condition was estimated, using the data of Reference 18, to be only about 5% of that measured at  $5100\text{\AA}$ .

The radiation profiles obtained in the spectral scan measurements with air as carrier gas have thus not been reconciled as to accountability for the behavior observed. Notwithstanding, the apparent pressure-broadened line width of the  $5106\text{\AA}$  copper line in air at 90.3 atm. was evaluated as follows. The scan data for pure air and air + Cu were used together (e.g., Figure 16) in order to subtract the continuum-like background radiation from the Cu-line scan profile. The half width at half height thus measured for the "net profile" Cu line scan of Figure 13(b) was  $0.52\text{\AA}$ . An estimate for  $\gamma_{oi}$  ( $i = \text{N}_2$ ) in Table 2, indicates a corresponding  $\gamma_{oi} = 0.021\text{\AA}$ , suggesting similar  $\rho_i$  values for  $\text{N}_2$  and air. Clearly, however, in view of the effects of the unknown background

16. DeVos, J.C., A New Determination of the Emissivity of Tungsten Ribbon, *Physica XX*, 690, (1954).
17. Wurster, W.H. and Marrone, P.V., Study of Infrared Emission in Heated Air, Cornell Aero. Lab. (now Calspan) Report No. QM-1373-A-4, July 1961.
18. Wurster, W.H., Measured Transition Probability for the First-Positive Band System of Nitrogen, *J. Chem. Phys.*, 36, 2111, April 1962.

radiation on the air-carrier measurements, observations cannot be quantified reliably. It is noted only, that to within the approximations implied above, there is no apparent effect of  $O_2$  on the  $5106\text{\AA}$  line width. No "net profile" half width estimate for the 45 atm case of Figure 13(a) could be considered since the diagnostic air-only runs were performed for the 90.3 atm. case only.

The ratio of the output signals of the  $5106\text{\AA}$  line opacity monitor in the air experiments were measured to be about 1.4 for air + Cu and 1.35 for air without Cu, at the 90.3 atm. test condition. The reflecting/non-reflecting wall channel signals were also in the ratio of 1.4 for the lower pressure (45.8 atm.) air + Cu run condition. These opacity measurements therefore indicate that the Cu line-width measurements in air were also performed under non-thin radiation conditions. As noted previously, however, in the discussion of the measured Cu line widths in the  $N_2$  + Cu experiments (Sec. 5.3.1), seriously-questioned reliability must be ascribed to the opacity-monitor data obtained during the line-width measurements. (See the post-test observations reported at the end of this section).

Two-channel radiometer measurements for the relative intensity,  $R$ , of the  $5153/5106\text{\AA}$  copper lines were also recorded during the shock tube experiments in air. In the absence of the copper aerosol, the  $R$  value measured in pure air was unity. The  $5106\text{\AA}$  radiometer channel record for this run is that shown in Figure 13(b). This result is, in fact, one to be expected for the response of the radiometer systems to a continuum source wherein negligible change in spectral radiance occurs over  $\sim 50\text{\AA}$ , the wavelength separation of the  $5153\text{\AA}$  and  $5106\text{\AA}$  radiometer channels.

The relative intensity of the  $5153\text{\AA}$  and  $5106\text{\AA}$  radiometer channels measured during the air + Cu experiments at 90.3 atm., corresponded to the large value,  $R = 0.56$ , at  $4970^\circ\text{K}$ . The corresponding data records are those shown in Figure 14. This result is one clearly compromised by the effect of the continuum-like background radiation contributions. However, since the respective channel signal levels measured in air without copper were the same (i.e.,  $R = 1$ ), the effect of subtracting this air-only radiation level as a

background signal correction common to the Air + Cu radiometer channel data could be investigated. The ratio of the net 5153Å and 5106Å signal intensities for air + Cu then yielded a value of  $R = 0.14$ , for the 90.3 atm., 4970°K test condition.

Reference to Figure 8 indicates that after making this large correction, the above  $R$  value is also close to the curve (of prescribed temperature dependence) whose location was defined by the optically thin relative transition probability measurements at 4000°K. The agreement for the air + Cu  $R$  value at 5000°K is, in fact, comparable to that already indicated on Figure 8 for the  $N_2$  + Cu data at  $\sim 6000^\circ\text{K}$ .

A final, post-test, observation should be made concerning the opacity-monitor data. This instrument was designed for use during the relative transition probability measurements for the purpose of confirming experimental operations under optically thin conditions. However, for the line width measurements, the opacity monitor measurements were considered as qualitative only. In particular, the two-channel system balance for this instrument was not checked during the course of the line width measurements. However, following the data analyses reported herein, the opacity monitor channel gain balances were subsequently checked, in view of the apparent contradictory indications of the radiometer relative intensity ratio data and the opacity monitor data. The opacity instrument channel gains were found to be out of balance, from unity, by 20%, in a direction that would require the opacity signal ratio data to be increased by a factor of 1.2.

Owing to the fact that such an instrument calibration measurement was not performed prior to, nor during the line width measurements, retroactive application of such a correction is not proposed. However, this finding does support previous conclusions that the opacity monitor data obtained during the line width measurements were unreliable and that the line width experiments were, in fact, performed closer to optically thin conditions.

## SECTION VI

### CONCLUSIONS AND RECOMMENDATIONS

#### 6.1 CONCLUSIONS

Relative transition probability measurements for the 5153Å and 5106Å copper atomic lines have been performed under optically thin conditions in argon, at a temperature of 4000°K. The measured relative intensity ratios,  $R$ , for the two copper lines defined the location of an experimental curve of  $R$  vs  $T$ . The temperature dependence of the curve was that calculated for the 5153/5106Å line intensity ratio, (Eqn. (8)), with the constant  $(g_u A)_{5153}/(g_u A)_{5106}$  fitted to the experimental determination at 4000°K. The  $R$  values measured at 4000°K were found to be in reasonably close accord with the results of Kock and Richter.<sup>12</sup>

Relative copper line intensity measurements were also obtained, using much more copper, as complementary data to the 5106Å copper line measurements performed in  $N_2$  and air. The two-channel radiometer measurements in  $N_2$ , at a temperature near 5900°K, were also found to yield  $R$  values which were reasonably close to the curve defined by the optically thin results. Complementary measurements using different path lengths (opacity monitor) indicated that the gas was optically thick, and it was not possible to reconcile these contradictory results. Post-test observations indicated, however, that the opacity-monitor data for the line-width measurements are not reliable.

Relative intensity measurements were also obtained in air at a temperature near 5000°K. These data, however, were superimposed upon a high level of background radiation within the radiometer filter bandpasses. On the basis of supplementary two-channel radiometer measurements performed in air without copper, however, a correction for the background radiation could be investigated for one of the test conditions in air. After making this large correction, the relative intensity ratio for the copper lines was then also found to exhibit close correlation with the measured  $R$  values at 4000°K and 5900°K.

The effect of pressure broadening on the 5106Å copper line was investigated in the shock tube experiments using both N<sub>2</sub> and air as Cu-aerosol carrier gases. Spectral scans of the 5106Å line in N<sub>2</sub> exhibited an increase in the measured line width which was consistent with the two-fold increase in total gas pressure. The measured half width at half height for the 5106Å Cu line, reduced to standard temperature and pressure conditions, was 0.021Å. The corresponding optical collision diameter was 5.7Å, which is close to the value reported by Ovechkin and Sandrigailo.<sup>(8)</sup> Similar spectral scan measurements of the 5106Å Cu line in air, however, were compromised because of a high level of underlying continuum-like radiation within the wavelength intervals of interest. This background radiation was shown to originate from the heated air carrier gas. No higher-order spectral contributions from shorter-wavelength radiation systems are believed to be responsible. Estimates were also made of the radiation, contributing within the band, from two of the principal radiation systems in high-temperature air. The estimated contributions from NO<sub>2</sub> radiative recombination and the N<sub>2</sub> first-positive system, however, were found not to be significant.

On the basis of supplementary spectral scan measurements performed in air without copper, a correction for the background radiation was made to the 5106Å Cu line scan data in Cu-seeded air at 90.3 atm. To first approximation, the "net profile" data for air as broadening gas indicated no effect due to the presence of O<sub>2</sub>, when compared with the N<sub>2</sub>-carrier data.

The 5106Å line center was observed to be shifted to longer wavelength with increase in N<sub>2</sub> gas pressure. The observed ratio of line full width at half height to line center shift was found to be in reasonable accord with Lindholm's<sup>(9)</sup> theoretical value for van der Waal forces and in agreement with the ratio measured by Ovechkin and Sandrigailo<sup>(8)</sup> for the 5106Å copper line in collisions with N<sub>2</sub> molecules.

The radiation behavior observed in the air aerosol-carrier gas experiments has not been resolved. Nor was it possible to pursue its diagnostic investigations further within the means of these studies. Also, in view of the significant effect of the underlying radiation on the 5106Å copper line spectral scan measurements in air, and the extent of corroborative shock tube checkout experiments required following readjustment of the spectrometer grating, it was not considered technically justifiable to proceed with similar spectral scans of the 5153Å copper line.

## 6.2 RECOMMENDATIONS

Because air is the test medium of primary interest in the AFFDL RENT experiments, it is expected that the contributions of radiating systems from the high-temperature air that have been observed herein will similarly compromise non-ambiguity in the interpretation of the Cu line intensity measurements in that facility.

The computational model for the development of an algorithm to deduce temperature from the Cu line intensity ratio must necessarily take into account all the factors which affect the operational measurement: the Cu loading, stagnation pressure levels, wavelength bandpass widths and positions, background assessment and compensation and flow non-uniformity in the region of measurement. In addition, the data which determine the basic physical parameters which are used in the model should be obtained with the same level of precision as will characterize the final operational measurement. Thus, there is a distinct advantage in using the same optical system for both the diagnostic development and the operational application.

The results of the present experiments have highlighted some of the complications that can arise with a simplified modeling approach based only on the consideration of idealized copper radiation. The summary recommendation, therefore, is that the optical system as presently configured at AFFDL be interfaced with a known, well-defined and uniform source of Cu-seeded, shock-heated air. In this way, the optical system can be calibrated with all uniform-flow radiation phenomena taken into account. The test times are compatible, because the frequency response of the system is high, having been designed to accommodate the rapid fluctuations known to exist in the arc facility. Additionally, the effects of the variation of wavelength bandpasses and position could be directly assessed and optimized.

# REFERENCES

1. Wurster, W.H., Shock-Tube Spectroscopy of Ablative Species, Proc. Sixth International Shock Tube Symposium, Freiburg, Germany, April 1967, Physics of Fluids Supplement, 12, I-92, May 1969.
2. Falk, T.J., Evaporation of Submicron Platinum Particles in a Shock Tube, J. Chem. Phys. 48, 3305, April 1968.
3. Wurster, W.H., Uranium-Oxygen Radiation Studies, Final Report, DNA 3398F, Calspan Corporation 1974.
4. Russo, A.L. and Wurster, W.H., Transition Probability and Pressure Broadening Parameters of Copper Atomic Lines, Interim Technical Report, Calspan Report No. WB-5726-A-2, January 1976.
5. Boyer, D.W., Russo, A.L. and Wurster, W.H., Transition Probability and Pressure Broadening Parameters of Copper Atomic Lines, Interim Progress Report, 1 January 1977 - 15 February 1977.
6. Corliss, C.H. A Review of Oscillator Strengths for Lines of CuI. Journal of Research-A. Physics and Chemistry, 74A, No. 6, 781, (1970).
7. Bader, Jon B., Time-Resolved Absolute Intensity Measurements of the 5106 Angstrom Copper Atomic Spectral Line in the AFFDL RENT Facility, AFFDL Technical Report TR-75-33, June 1975.
8. Ovechkin, G.V. and Sandrigailo, L.E. Line Broadening and Shift in a Arc for Low Copper Contents, J. Applied Spectroscopy (USSR), 10, 565, April 1969.
9. Lindholm, E., Arkiv Mat. Astr. Fys., 28B, No. 3 (1941)
10. Ludwig, C.B., Malkmus, W., Reardon, J.E. and Thomson, J.A. Handbook of Infrared Radiation From Combustion Gases. NASA SP-3080, (1973).
11. Kostkowski, H.J. and Bass, A.M. Slit Function Effects in the Direct Measurement of Absorption Line Half-Widths and Intensities. J. Opt. Soc. Am., 46, 1060, December 1956.
12. Kock, M. and Richter, J., Experimental Transition Probabilities and the Solar Abundance of Copper, Zeitschrift Fur Astrophysik, 69, 180, (1968).
13. Corliss, C.H. and Bozman, W.R., Experimental Transition Probabilities for Spectral Lines of Seventy Elements, NBS Monograph 53, (1962).
14. Allen, R.A., Air Radiation Tables: Spectral Distribution Functions For Molecular Band Systems, AVCO Everett Research Report No. 236, April 1966.

15. Treanor, C.E. and Wurster, W.H., Measured Transition Probabilities for the Schumann-Runge System of Oxygen, J. Chem. Phys. 32, 758, 1960.
16. DeVos, J.C., A New Determination of the Emissivity of Tungsten Ribbon, Physica XX, 690, (1954).
17. Wurster, W.H. and Marrone, P.V., Study of Infrared Emission in Heated Air, Cornell Aero. Lab. (now Calspan) Report No. QM-1373-A-4, July 1961.
18. Wurster, W.H., Measured Transition Probability for the First-Positive Band System of Nitrogen, J. Chem. Phys., 36, 2111, April 1962.